



Tectonics

RESEARCH ARTICLE

10.1002/2015TC004000

Key Points:

- Reconstruction of the topographic evolution of the Ethiopian Plateau
- The present-day topographic dome is a long-term feature present since the Oligocene
- Much of the topography has been and is dynamically sustained

Supporting Information:

- Figures S1–S10 and Tables S1–S3

Correspondence to:

A. Sembroni,
andrea.sembroni@uniroma3.it

Citation:

Sembroni, A., C. Faccenna, T. W. Becker, P. Molin, and B. Abebe (2016), Long-term, deep-mantle support of the Ethiopia-Yemen Plateau, *Tectonics*, 35, 469–488, doi:10.1002/2015TC004000.

Received 6 AUG 2015

Accepted 4 FEB 2016

Accepted article online 8 FEB 2016

Published online 29 FEB 2016

Long-term, deep-mantle support of the Ethiopia-Yemen Plateau

Andrea Sembroni¹, Claudio Faccenna¹, Thorsten W. Becker², Paola Molin¹, and Bekele Abebe³

¹Department of Science, Roma Tre University, Rome, Italy, ²Department of Earth Sciences, University of Southern California, Los Angeles, California, USA, ³Department of Earth Sciences, School of Earth Sciences, Addis Ababa, Ethiopia

Abstract Ethiopia is a key site to investigate the interactions between mantle dynamics and surface processes because of the presence of the Main Ethiopian Rift (MER), Cenozoic continental flood basalt volcanism, and plateau uplift. The role of mantle plumes in causing Ethiopia's flood basalts and tectonics has been commonly accepted. However, the location and number of plumes and their impact on surface uplift are still uncertain. Here we present new constraints on the geological and topographic evolution of the Ethiopian Plateau (NW Ethiopia) prior to and after the emplacement of the large flood basalts (40–20 Ma). Using geological information and topographic reconstructions, we show that the large topographic dome that we see today is a long-term feature, already present prior to the emplacement of the flood basalts. We also infer that large-scale doming operated even after the emplacement of the flood basalts. Using a comparison with the present-day topographic setting, we show that an important component of the topography has been and is presently represented by a residual, nonisostatic, dynamic contribution. We conclude that the growth of the Ethiopian Plateau is a long-term, probably still active, dynamically supported process. Our arguments provide constraints on the processes leading to the formation of one of the largest igneous plateaus on Earth.

1. Introduction

The surface of the Earth is sculpted by a combination of processes, occurring in the crust, the lithosphere, and, at greater depth, in the mantle [e.g., Molnar and England, 1990; Gurnis, 2001; Wobus et al., 2006; Boschi et al., 2010; Braun, 2010; Burbank and Anderson, 2011; Molin et al., 2011; Braun et al., 2013]. Isostasy is considered as the main controlling process, explaining a large part of the topographic signal in the continents and in the oceanic plates. In addition to the isostatic component of topography, another component may arise from density anomalies and resultant flow of the deeper mantle, what is commonly referred as dynamic topography [e.g., Hager et al., 1985; Lithgow-Bertelloni and Silver, 1998; Gurnis et al., 2000; Daradich et al., 2003; Moucha et al., 2008; Boschi et al., 2010; Moucha and Forte, 2011; Faccenna et al., 2013; Becker et al., 2014].

Key examples to study the interaction and feedback between mantle dynamics and related topography are found in regions where a hot mantle upwelling is inferred to cause volcanoes and large igneous provinces (LIP). In those regions, dynamic topography may induce large-scale doming [e.g., Sengör, 2001], but the topography response to upwelling may be overprinted by preexisting relief and deformation in response to far-field stresses [Burov and Guillou-Frottier, 2005; Burov et al., 2007; Burov and Gerya, 2014]. Several models suggest that components of the African plate's high elevation are related to the effect of dynamic topography [Burke, 1996; Lithgow-Bertelloni and Silver, 1998; Ritsema et al., 1999; Gurnis et al., 2000; Daradich et al., 2003; Forte et al., 2010; Moucha and Forte, 2011; Faccenna et al., 2013] with a rate of change that depends on density and lateral/radial variations in viscosity [e.g., Gurnis et al., 2000], but its location, timing, and amplitude are still debated.

Ethiopia has long been recognized as a natural laboratory to study the interaction between mantle dynamics and surface processes because of the presence of the Main Ethiopian Rift (MER), Cenozoic continental flood basalt volcanism, and plateau uplift [Ebinger and Casey, 2001; Nyblade and Langston, 2002; Furman et al., 2006; Bastow et al., 2008]. Plateau uplift probably had a first order impact on climate, inhibiting circulation of moist air and then inducing aridification [Sepulchre et al., 2006]. The role of mantle plumes in causing Ethiopia's flood basalts and tectonics has been commonly accepted, even if the location and number of plumes or mantle upwellings are controversial [e.g., Schilling et al., 1992; Burke, 1996; Ebinger and Sleep, 1998; George et al.,

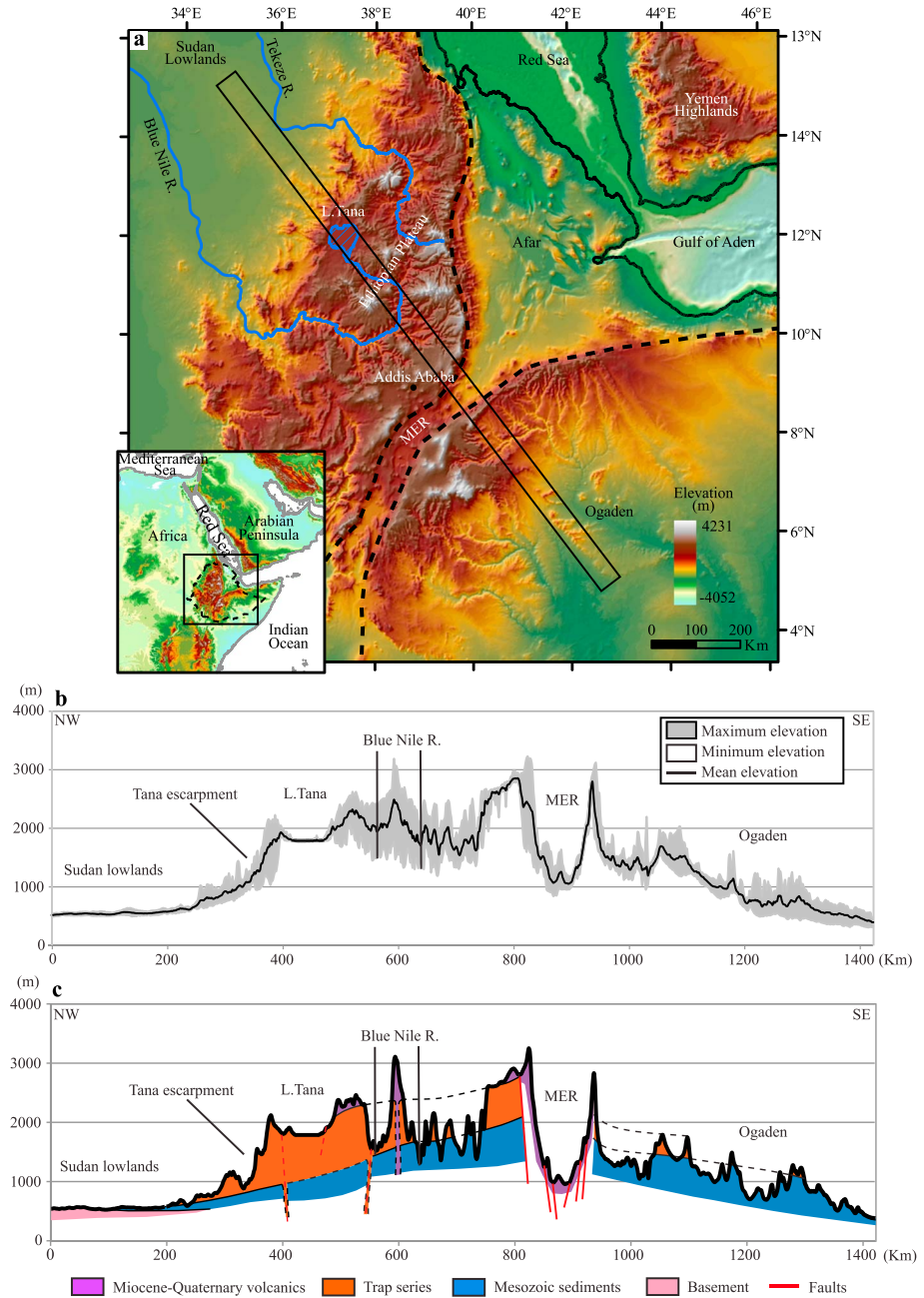


Figure 1. (a) Digital elevation model of Ethiopia (ETOPO1, resolution of ~2000 m). The black solid box in the inset shows the location of the study area with respect to Africa and Arabian Peninsula; the black dashed line indicates the Ethiopian national borders. The black solid rectangle shows (b) the trace of swath profile and (c) geological section.

1998; Courtillot et al., 1999; Rogers et al., 2000; Furman et al., 2006; Rogers, 2006]. The debates arise mainly from the uneven geophysical data coverage, the intrinsic limitations of global tomography studies, and the dependence of seismic velocity on other parameters (composition, phase) in addition to temperature [e.g. Corti, 2009]. Studies have proposed the existence of one [Ebinger and Sleep, 1998; Furman et al., 2006] or two plumes [George et al., 1998; Rogers et al., 2000] impinging the base of the continental lithosphere. Another source of uncertainty derives from the amount and timing of uplift. Ethiopia was a passive margin in the Mesozoic time and the marine sequences deposited along this margin provide regional markers to constrain uplift. The Ethiopian Plateau presents an almost flat physiography with an average elevation of 2500 m asl (above sea level). This configuration may have been attained before [Sengör, 2001], during [Pik et al., 2003],

or after [Gani *et al.*, 2007] the emplacement of the flood basalts or both. Understanding the timing and amount of uplift of the region can constrain the processes leading to the high plateau.

This study provides new constraints on the topographic evolution of the Ethiopian Plateau prior to and after the emplacement of widespread flood basalts between ~40 and 20 Ma. Using geological information and topographic reconstructions, we show that the large topographic dome that we see today is probably a long-term, dynamically supported feature.

2. Geological Setting

To first order, the topography of Ethiopia is dome shaped (Figure 1b). The dome has a maximum elevation of ~2500 m (around Addis Ababa) and a diameter of ~1200 km. This feature is crosscut by the Main Ethiopian Rift (MER), located immediately east of the dome's apex (Figure 1b). The timing and the uplift rate of the dome have been widely discussed [e.g., *Ebinger et al.*, 1989; *Ebinger and Hayward*, 1996; *Sengör*, 2001; *Pik et al.*, 2003; *Mackenzie et al.*, 2005; *Tiberi et al.*, 2005; *Cornwell et al.*, 2006, 2010; *Pérez-Gussinyé et al.*, 2006; *Gani et al.*, 2007; *Bastow et al.*, 2008]. Early works suggested the uplift to be Upper Eocene in age [*Dainelli*, 1943; *Beydoun*, 1960; *Mohr*, 1962; *Sengör*, 2001]. Later studies [e.g., *Mohr*, 1967; *Merla et al.*, 1979] inferred a more complex history of uplift and volcanism during the Tertiary [e.g., *Baker et al.*, 1972; *McDougall et al.*, 1975; *Berhe et al.*, 1987]. From gravity-isostasy relations, *Ebinger et al.* [1989] inferred that East Africa plateau topography is dynamically maintained by convection within the asthenosphere. *Sengör* [2001], by reconstructing the top and base surfaces of Eocene continental deposits in the Arabian Peninsula, inferred a tilting of the formations and calculated a minimum surface uplift of ~1200 m. Such uplift has been related to the impinging of Afar plume at the base of the lithosphere that occurred in the Eocene [*Sengör*, 2001] prior to LIP emplacement. *Pik et al.* [2003], based on thermochronological and morphological analysis on the Blue Nile drainage system, argued that erosion initiated in the Blue Nile canyon as early as 25–29 Ma and that the elevated plateau physiography existed since the Late Oligocene. *Pérez-Gussinyé et al.* [2006] and *Ebinger and Hayward* [1996] considered flexural uplift of rift shoulders as a process that creates topography. *Tiberi et al.* [2005], *Cornwell et al.* [2006], and *Bastow et al.* [2008] demonstrated that crustal underplating is one of the major contributors to uplift in Ethiopia. *Gani et al.* [2007], using incision rates along the 1.6 km deep Blue Nile gorges, identified three different phases of uplift since ~29 Ma.

The Ethiopian Plateau is located in the northwestern sector of Ethiopia (Figure 1a). It is confined on the western and eastern sides by the Tana and Afar escarpments, respectively (Figure 2b). The Tana escarpment develops on the western side of Lake Tana and is an erosional feature formed by scarp retreat [*Jepsen and Athearn*, 1961; *Chorowicz et al.*, 1998; *Gani et al.*, 2008]. Lake Tana is located in the western portion of the plateau and lies at the convergence of three Mesozoic grabens: Debre Tabor from the east, Gondar from the north-northwest, and Dengel Ber from the south-southwest [*Chorowicz et al.*, 1998; *Hautot et al.*, 2006]. The Afar escarpment is generated by the rift formation and related footwall uplift [*Weissel and Karner*, 1989; *Weissel et al.*, 1995]. The Ethiopian Plateau is drained by two main rivers: the Blue Nile and the Tekeze, from the south and north, respectively (Figure 2b).

The Ethiopian Plateau is covered by extensive Eocene-Miocene (40–20 Ma) [*Zumbo et al.*, 1995; *Baker et al.*, 1996; *Hofmann et al.*, 1997; *Rochette et al.*, 1998; *Ebinger*, 2005] continental flood basalts, 500–1500 m in thickness [*Minucci*, 1938; *Jepsen and Athearn*, 1961; *Mohr and Zanettin*, 1988] (Figures 2a and 3c). Such deposits covered an area of $\sim 1 \cdot 10^6$ km² [*Mohr*, 1983; *Rochette et al.*, 1998], from Ethiopia up to Eritrea and Yemen regions (Figures 2a and 3c). They overlie an alternation of Mesozoic sandstones and limestones (~3 km in thickness) [*Cornwell et al.*, 2010]. Such formations deposited into NW-SE striking structural basins formed by the extensional deformation associated to Karoo-type rifts (Early Permian) (see *Guiraud et al.* [2005] for review). In the Mesozoic continental rifting was very active within the African plate, giving rise to several NW-SE narrow troughs, as documented by the Blue Nile, Malut and Muglad rifts in Sudan, and by the Anza graben in Southern Ethiopia and Northern Kenya [*Corti*, 2009] (see Figure 3d). The Mesozoic sediments are unconformably located on a crystalline basement [*Kebede*, 2013] (Figure 2a). Basement rocks are part of the Arabian-Nubian Shield and record folding, compression, and metamorphism due to the collision between east and west Gondwana [*Stern*, 1994]. The flood basalt eruption occurred through fissures [*Mohr and Zanettin*, 1988] mostly controlled by Precambrian and Mesozoic zones of weakness [*Mege and Korme*,

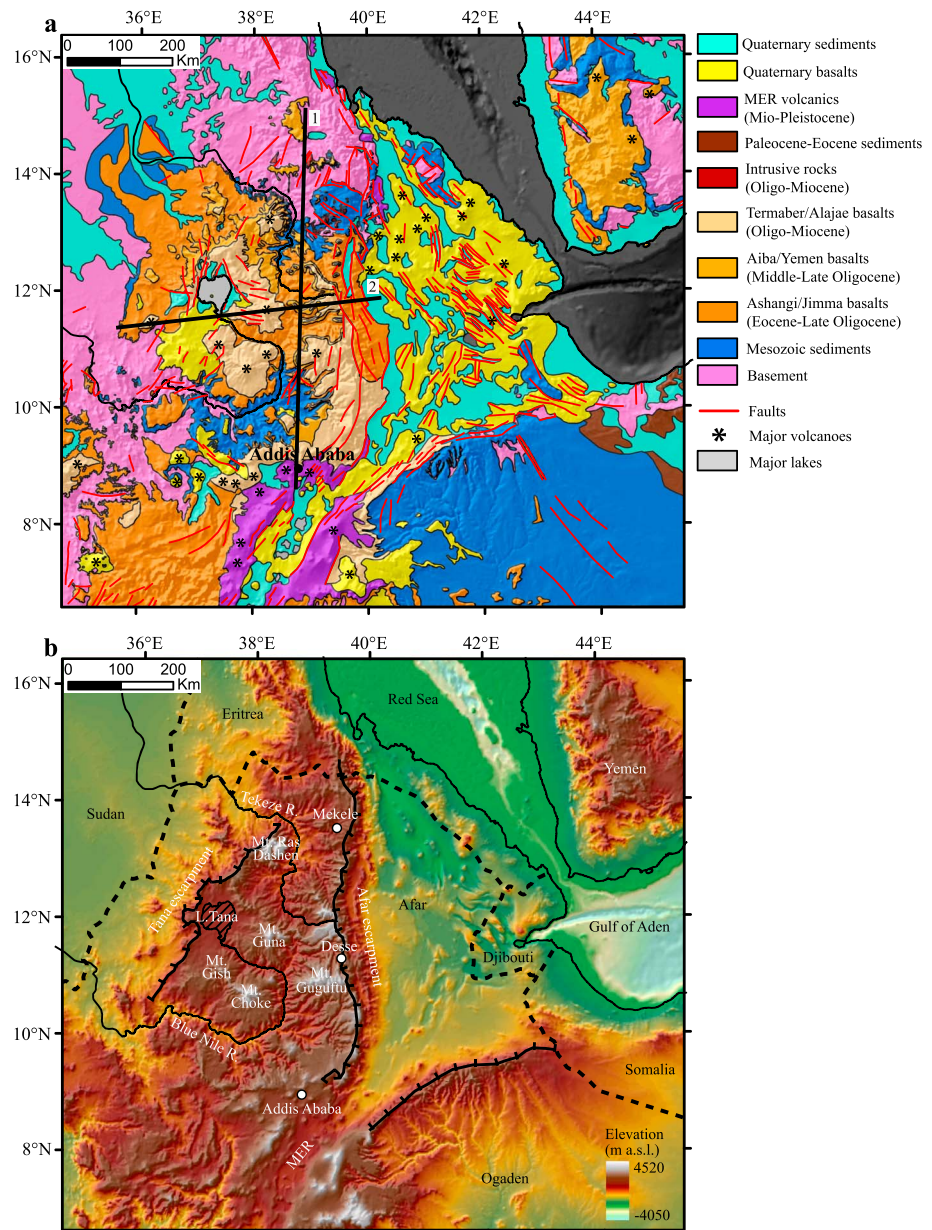


Figure 2. (a) Geological map of the study area compiled from the 1:2,000,000 scale geological map of Ethiopia/Sudan border [Tefera, 1996; G.M.R.D., 1981], the 1:1,500,000 scale geological map of Yemen [As-Saruri, 2004], and the available 1:250,000 scale maps of Ethiopia [Hailu, 1975; Kazmin, 1976; Garland, 1980; Tsige and Hailu, 2007; Chumburo, 2009; Zenebe and Mariam, 2011]. The map is draped over the shaded topography. The black solid lines indicate the traces of the geological sections (Figures 3a and 3b); (b) topographic configuration of the study area (ETOPO1); the black dashed lines represent the national borders while the black solid lines indicate the rift and Tana escarpments.

2004]. This event was probably concomitant with the Red Sea-Gulf of Aden continental rifting (Late Oligocene) [Wolfenden et al., 2005] but predates the development of the MER (Late Miocene) [Wolfenden et al., 2004; Bonini et al., 2005]. The location of the fissures system is still uncertain. Five hundred meter thick basalts as old as 45 Ma have been described in southern Ethiopia separating the MER from the Kenya rift [Davidson and Rex, 1980; Ebinger et al., 1993; George et al., 1998]. The chemical composition of the flood basalts supports a magma genesis from a broad region of mantle upwelling, heterogeneous in terms of temperature and composition [Kieffer et al., 2004].

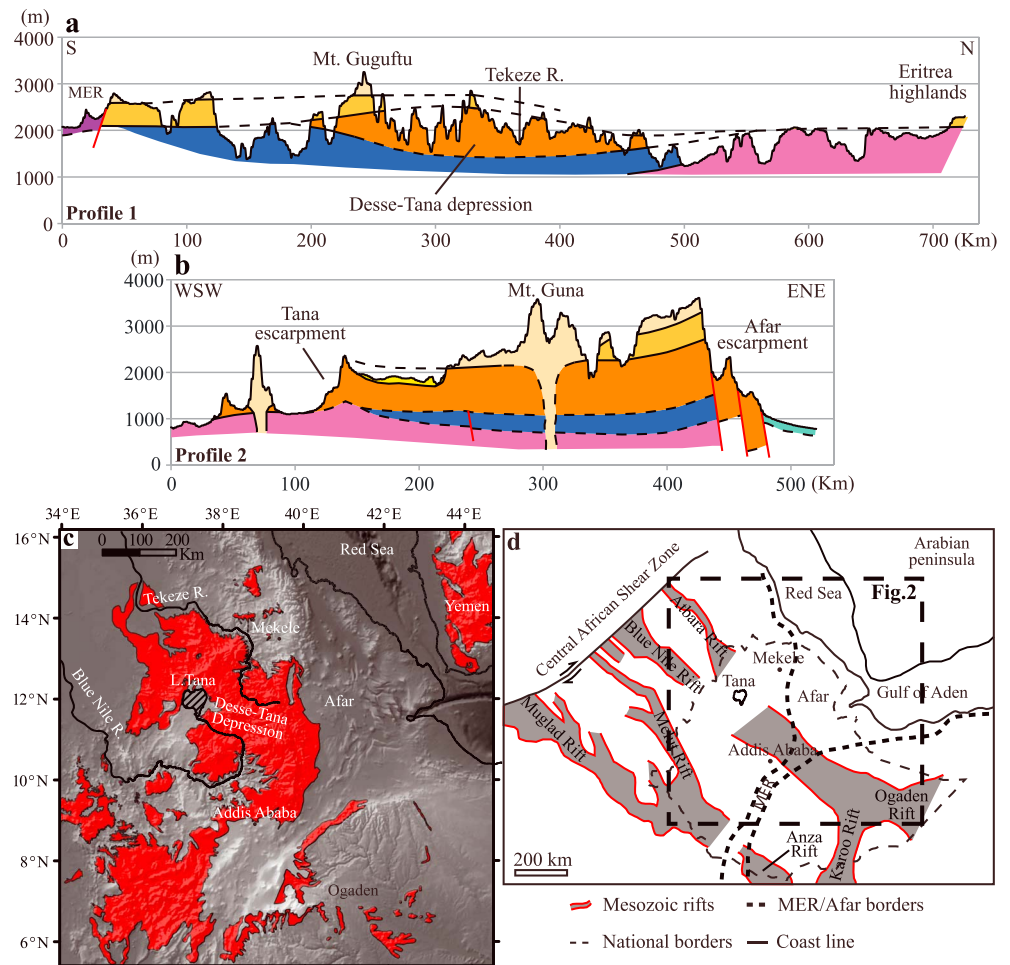
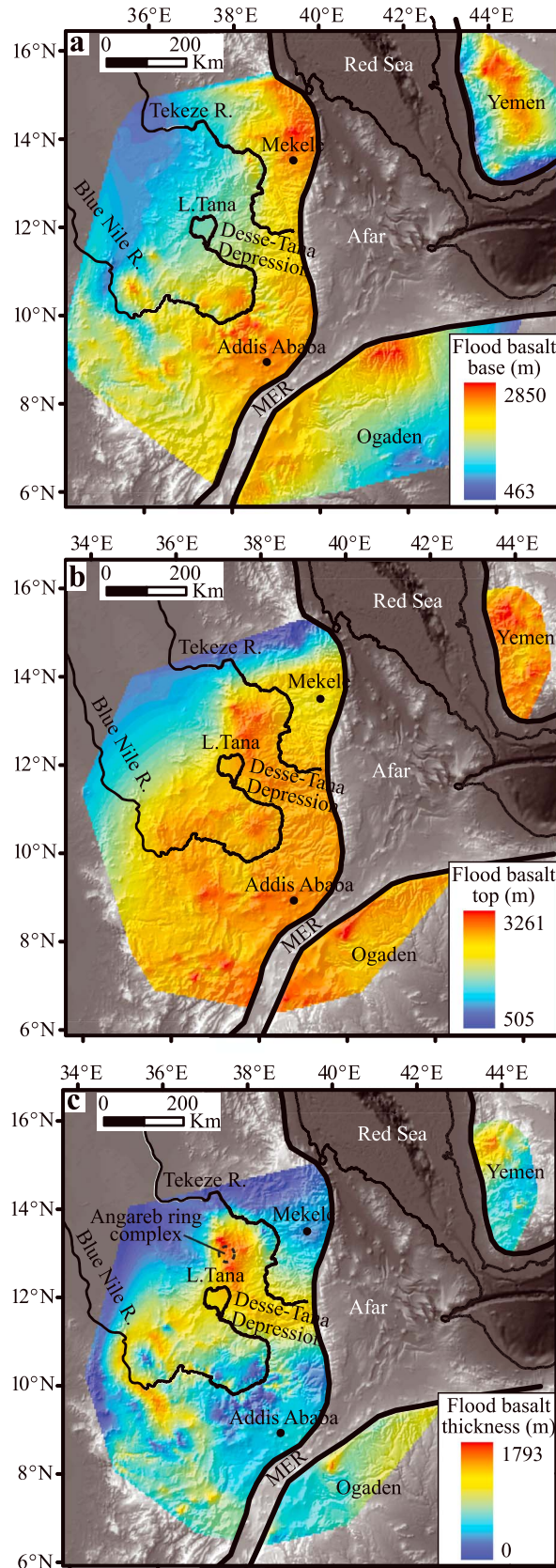


Figure 3. (a, b) Geological sections inferred from Figure 2a; (c) map of the flood basalt outcrops; (d) NW-SE trending Mesozoic rift basins developed in Ethiopia and surrounding areas (modified after Gani *et al.* [2008] and Corti [2009]); the black dashed box delimits the area of Figure 2.

Immediately after the peak of flood basalt emplacement, a number of large shield volcanoes developed from 30 Ma to ~10 Ma on the surface of the basaltic plateau [Kieffer *et al.*, 2004] rising 1000–2000 m above the original plateau surface [Mohr and Zanettin, 1988; Kieffer *et al.*, 2004] (Figure 2). In the early Miocene [Hagos *et al.*, 2010; Natali *et al.*, 2013] the northernmost sector of Ethiopian Plateau experienced an intense magmatic activity with the formation of huge intrusive bodies (Adwa Plugs and Mekele Dolerite; Figure 2a). Since the late Pliocene, magmatic and tectonic activities moved mainly into the axial sector of the rift and in the Afar depression [Ebinger, 2005].

3. Geometry of the Flood Basalts

We use geological information to reconstruct the topography prior to and after the emplacement of the flood basalt deposits. We reconstruct the geometry of the basalts over the Ethiopian, Somalian, and Yemen Plateaus, using several geological maps from the literature [Pik *et al.*, 1999; Kieffer *et al.*, 2004; Abbate *et al.*, 2015], 1:250,000 scale geological maps and field control over Ethiopia [Hailu, 1975; Kazmin, 1976; Garland, 1980; Tsige and Hailu, 2007; Chumburo, 2009; Zenebe and Mariam, 2011], a 1:2,000,000 scale geological map on the Ethiopia-Sudan border [Geological And Mineral Resources Department, 1981; Tefera *et al.*, 1996], and a 1:1,500,000 scale geological map over Yemen [As-Saruri, 2004]. We process all the data in geographic information system using ETOPO1 [http://www.ngdc.noaa.gov/] for elevation. We trace the flood basalt base surface mapping the contact with the sedimentary and metamorphic basement (see Figure S1 in the



supporting information) and interpolate points by a nearest-neighbor triangulation algorithm. We reconstruct the flood basalt top surface by basaltic plateau remnants. They appear all over Ethiopia and Yemen highlands between an elevation of 2400 and 2600 m asl (above sea level) and consist of flat or gently sloping (1–2°) surfaces bounded by steep slopes. Using geological maps and a digital elevation model (DEM) analysis, we select all the remnants and interpolate them. The prerift deposits are obscured everywhere within the Ethiopian and Afar rifts, except for the Danakil and Guraghe areas. We do not take into account such spots in our analysis because in both cases the contact Trap sedimentary basement is not visible at the scale of analysis or it is mainly a tectonic contact. By subtracting the flood basalt base surface from the top one, we derive the flood basalt thickness map. Figure 4 shows the results of this analysis, described in the following paragraphs.

1. The present-day base of the flood basalts follows the large-scale structure of the topographic dome and shows an undulating topography ranging from 463 to 2850 m (Figures 1c and 4a). The highest sectors are the areas close to Mekele and Addis Ababa along the western side of the MER and the Ogaden and Yemen regions on the southern and eastern side of the rift, respectively (Figure 4a). On the western side, the Mekele and Addis Ababa highs are separated by a smooth and wide depression oriented NNW-SSE and extending from Desse to Lake Tana (Desse-Tana Depression). Figures 3a and 4a best illustrate this feature which presents an irregular, almost triangular shape: the width ranges from 200 to 400 km, while its depth increases from 600 m to 1000 m to the NW.
2. The top of the basalts runs at an average altitude of 2500 m (Figure 4b). High ele-

Figure 4. Maps of (a) the flood basalt base and (b) top surfaces traced by mapping respectively the flood basalts-sedimentary basement contact and the basaltic plateau remnants (not corrected from the flexural uplift at Afar and Tana escarpments); (c) map of the flood basalt thickness elaborated by subtracting the flood basalt base surface from the top one.

vations of the top surface (between 2500 and 3261 m) are concentrated under the volcanoes, which preserve the original basalt thickness from erosion and along the eastern portion of the Ethiopian Plateau. The shoulders of the rift are always uplifted, deforming the basalts since Late Miocene [Weissel *et al.*, 1995; Wolfenden *et al.*, 2004; Bonini *et al.*, 2005].

3. The flood basalt thickness map shows an asymmetrical distribution with respect to the Afar depression and the rift valley (Figure 4c). Most of the entire volume forms the Ethiopian Plateau and concentrates in the Lake Tana region. In particular, the highest values fall around the Angareb ring complex, immediately north of the lake (Figure 3c). This region most probably represented one of the main feeding areas of the system [Hahn *et al.*, 1977]. Thick deposits (1200–1500 m) fill the Dese-Tana Depression and are located in correspondence of the lower Blue Nile River valley (Figure 3c).
4. By considering the actual Trap distribution (Figure 3c) and thickness (Figure 4c) we estimate a minimum total Trap volume of $\sim 9 \cdot 10^5 \text{ km}^3$ (84% in the Ethiopian Plateau, 10% in the Somalian Plateau, and 6% in the Yemen Plateau). Such values are comparable to Rochette *et al.*'s [1998] estimate, $\sim 1.2 \cdot 10^6 \text{ km}^3$, which considers an average basalt thickness of 1.5 km and a circular areal distribution.
5. The flood basalts have been classified into several units according to chronological and stratigraphic criteria. In particular, Zanettin *et al.* [1980] distinguished two main volcanic stages: pre-Oligocene and Oligocene-Miocene. The first stage is characterized by the deposition of the Ashangi basalts (see Figure 2a). This unit covers all the northwestern sector of Ethiopia and limited areas of the Ogaden basin (Figure 2a). The precise age is still uncertain. However, considering the age of the overlying unit (Aiba basalts), Zanettin *et al.* [1980] located the Ashangi basalts in the Eocene. This unit is contemporaneous to the Jimma basalts which covered the southern sector of Ethiopia since Late Eocene [Davidson and Rex, 1980; Ebinger *et al.*, 1993; George *et al.*, 1998]. In Figure 2a both units have been represented by the same color. The Oligocene-Miocene stage is characterized by the deposition of three units: Aiba, Termaber, and Alaji basalts [Zanettin *et al.*, 1980]. This volcanism occurred over the whole central Ethiopian and Somalian Plateau between 32 and 13 Ma [Zanettin *et al.*, 1980], and it is associated mainly to the shield volcanoes (Semien Mountains, Mount Guna, Mount Choke, and Mount Guguftu; Figure 2b) activities [Kieffer *et al.*, 2004]. Such basalts are contemporaneous to the Yemen Trap Series which range in age from 31 to 16 Ma [Bosworth *et al.*, 2005] with the peak of the volcanic activity comprising between 30.9 and 26.5 Ma [Mattash *et al.*, 2013]. For this reason, the Aiba basalts and Yemen Traps have been represented by the same color in Figure 2a. Geological sections (Figures 3a and 3b) show that the Ashangi basalts fill depressions such as the Dese-Tana Depression (average thickness of 1000 m), pinching out onto the basement units while the Oligocene-Miocene stage basalts (average thickness of 500 m) simply flowed onto the Ashangi ones reaching the Eritrea region (Figure 3a).

Summing up, the analysis of the flood basalts shows that at the time of the flood basalt emplacement there was already a morphological relief, with topographic highs and troughs and that after the emplacement of the basalts, the entire region upraised forming a large-scale domal structure.

4. Restoring Topography Back in Time

Here we illustrate the topography reconstruction prior to and after the emplacement of the flood basalts, accounting for the contribution of flexural (un)loading.

4.1. Flexural (Un)Loading

To restore the topographic structure prior to rifting, it is necessary to estimate the flexural response due to the tectonic unloading along the rift shoulder (Late Miocene) [Wolfenden *et al.*, 2004; Bonini *et al.*, 2005] and to erosional unloading (since Late Oligocene) [Pik *et al.*, 2003; Gani *et al.*, 2007] at the base of the Tana escarpment. Following the approach of Weissel *et al.* [1995], we estimate 2-D surfaces in a 3-D space by interpolating near-parallel cross sections, transverse to the studied structures (Tana and Afar escarpments), assuming a cylindrical bending of the plate and ignoring subsurface loads.

We estimate the vertical displacement $w(x)$ of rift flanks as isostatic response to unloading of a broken lithosphere due to extension (see supporting information) as follows:

$$w(x) = w_0 e^{-x/\alpha} \cos \frac{x}{\alpha} \quad (1)$$

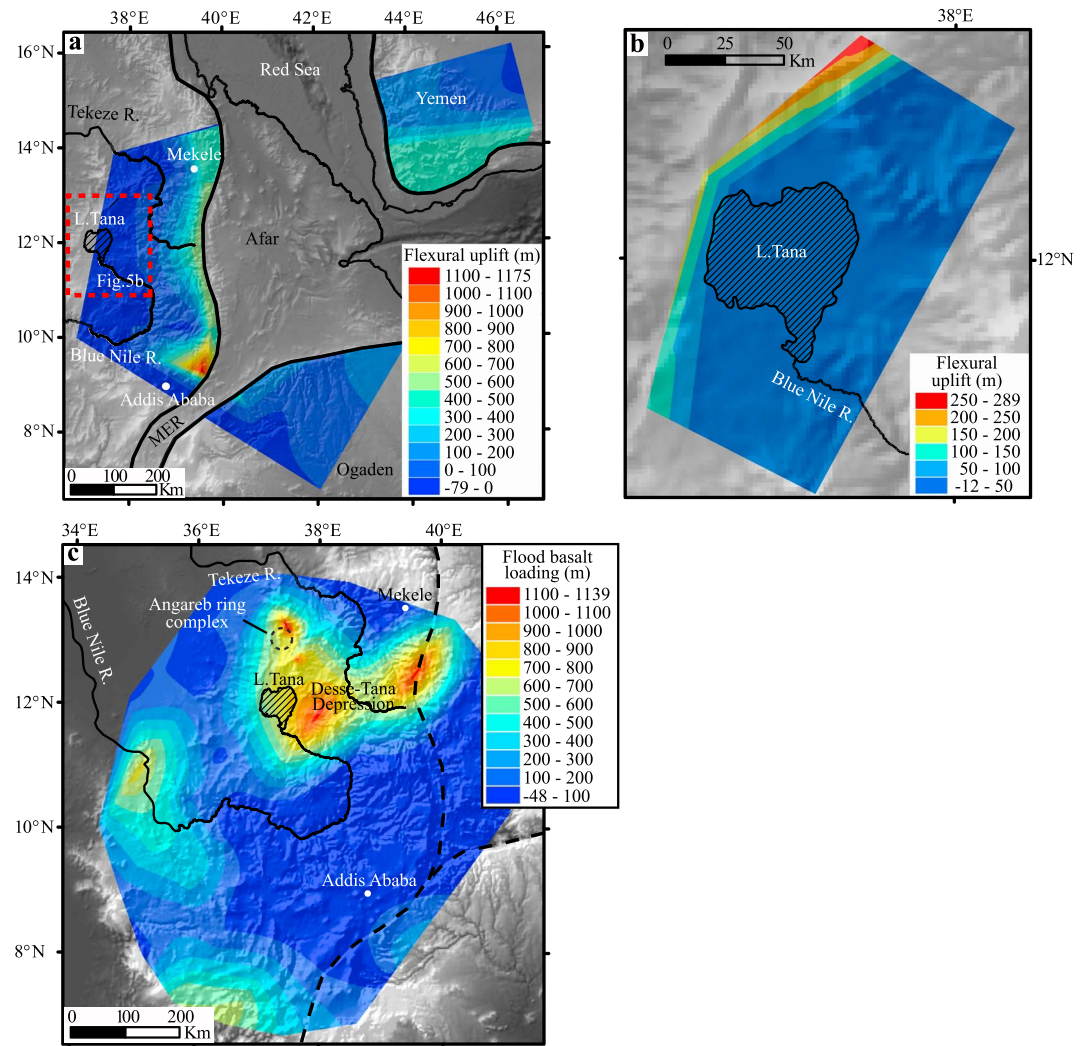


Figure 5. Maps of the areal distribution of flexural uplift along (a) the rift margins and (b) the Tana escarpment. The red dashed box indicates the area of Figure 5b; (c) map of the isostatic contribution due to basalt loading traced on the mosaic DEM (paleogeographic reconstruction of the Oligocene plates configuration based on the palaeotectonic maps of the Middle East by Barrier and Vrielynck [2008]); the black dashed lines indicate the plate boundaries.

where w_0 is the maximum vertical displacement caused by the flexure and α is the flexural wavelength [Turcotte and Schubert, 1982]. We fit the model curves with eight topographic profiles, extracted from smoothed topography (30 km in radius smoothing circular window), using an iterative, least squares Levenberg-Marquardt fitting algorithm (as implemented in Gnuplot, <http://www.gnuplot.info/>; see Figure S2 in the supporting information). The flexural model of the rift shoulders shows a deformation up to a distance of 200 km from the rift escarpments in agreement with Weissel *et al.* [1995] (Figure 5a). The maximum vertical displacement on the Ethiopian Plateau varies from ~430 m to ~1175 m (Figure 5a and supporting information).

In order to calculate the Tana escarpment maximum vertical displacement (w_0), related to the flexural unloading of the lithosphere due to erosion (see supporting information), we use the solution for the case of an unbroken lithosphere [Turcotte and Schubert, 1982]

$$w(x) = w_0 e^{-x/\alpha} \left(\cos \frac{x}{\alpha} + \sin \frac{x}{\alpha} \right) \quad (2)$$

As for the rift shoulders uplift, we fit the model curves with three topographic profiles (Figure S3). In this case, we extract the profiles from the observed topography instead of the smoothed one as the wavelength of

flexural uplift in this area is equal or smaller than the circular window radius used to smooth the present topography (30 km). The flexural model of the Tana escarpment caused the warping of basalt up to a distance of ~30 km from the escarpment. The flexural uplift ranges between 140 and 290 m (see Figure 5b and supporting information).

We also estimate the contribution due to flood basalt loading. The onset of flood basalts occurred between ~40 and ~20 Ma with the vast volume erupting at ~30 Ma [Zumbo *et al.*, 1995; Baker *et al.*, 1996; Hofmann *et al.*, 1997; Rochette *et al.*, 1998; Ebinger, 2005], coincident with opening of the Red Sea and Gulf of Aden (30–28 Ma) [Wolfenden *et al.*, 2005] and before the initiation of the MER (~11 Ma) [Wolfenden *et al.*, 2004; Bonini *et al.*, 2005]. For this reason, in order to better define the preflood basalt topography, we attempt a paleogeographic reconstruction of the Oligocene plates configuration (mosaic DEM) referring to the paleotectonic maps of the Middle East by Barrier and Vrielynck [2008]. Then, by using the flood basalt thickness map data (Figure S4), we calculate the flexural deformation due to flood basalt loading along eight profiles (see supporting information) and interpolate the resultant profiles by a nearest-neighbor triangulation algorithm (Figure 5c). The load of basalts caused a subsidence ranging between 116 and 1140 m and a bulging between 5 and 48 m (Figure 5c). The highest values are found immediately north of the Lake Tana in correspondence with the Angareb ring complex which, according to Hahn *et al.* [1977], represented one of the most active flood basalt eruption centers. From the erosional unloading model, we determine a maximum flexural uplift between 47 and 156 m (see supporting information Table S3 and Figure S5). Such an isostatic contribution can be considered negligible compared to the 2000 m of total uplift registered in the area [Pik *et al.*, 2003; Gani *et al.*, 2007].

Another contribution to topography comes from the crustal thickness variation, for example, as shown from the EAGLE seismic network profiles [Mackenzie *et al.*, 2005; Tiberi *et al.*, 2005; Cornwell *et al.*, 2006; Bastow *et al.*, 2008; Bastow *et al.*, 2011]. In particular, the crustal thickness decreases from 32 to 24 km along the rift axis from south to north [Tiberi *et al.*, 2005]. The values increase to more than 40 km beneath the Ethiopian Plateau [Tiberi *et al.*, 2005] where a ~15 km thick high-velocity lowest crustal layer has been inferred [Mackenzie *et al.*, 2005]. Such an anomaly has been associated with the Oligocene flood basalt eruption event with possible subsequent addition by recent magmatic activity [Mackenzie *et al.*, 2005]. The crust beneath the Somali Plateau presents lower values of ~35 km [Mackenzie *et al.*, 2005]. Beneath the Yemen Plateau the crust shows a thickness of ~35 km. The values decrease to ~22 km in coastal areas and reach less than 14 km on the Red Sea coast where presence of high-velocity syn-rift mafic intrusions in the lower crust has been inferred [Ahmed *et al.*, 2013]. By assuming Airy isostatic compensation for the crustal thickness variations observed throughout the study region and taking into account ~10 km of underplating, Tiberi *et al.* [2005] calculated ~500 m of Ethiopian Plateau dynamic uplift.

4.2. Postflood Basalt Topography

To reconstruct the topography of the large-scale doming as observed on the flood basalt base surface (Figures 1c and 4a), we smooth the flood basalt base surface (elaborated from the mosaic DEM; see Figure 6a), corrected from the flexural uplift at rift and Tana escarpments, by a low-pass filter. The low-pass filter technique is commonly adopted for topography analysis to isolate the long wavelength component, possibly related to mantle-scale features from crustal ones [e.g., D'Agostino and McKenzie, 1999; Molin *et al.*, 2004; Wegmann *et al.*, 2007; Roy *et al.*, 2009; Faccenna *et al.*, 2011; Molin *et al.*, 2011]. Figures 6b and 7b show the result of 200 km low-pass filter (methods and result for other filters are in Figure S6 in the supporting information). The resulting feature is a large topographic high (up to ~1700 m) elongating from Addis Ababa to Yemen with a NE-SW trend (Figures 6b and 7b). This large feature splits in two topographic highs (~2000 m) (corresponding to Addis Ababa and Yemen areas) decreasing the filter wavelength from 300 to 100 km (see Figure S6).

4.3. Preflood Basalt Topography

Subtracting the large-scale doming feature, the flood basalt loading and the flexural uplift contributions, we obtain a preflood basalt topography (Figures 7a and S7). The maps present similar configurations, with two topographic highs corresponding to the area between Addis Ababa and Mekele and to the southwestern portion of the study area (Figure S7). The first one is characterized by a maximum elevation of ~1300–1400 m and extends from Lake Tana to the east with a WSW-ENE trend. The second high extends with a NW-SE trend

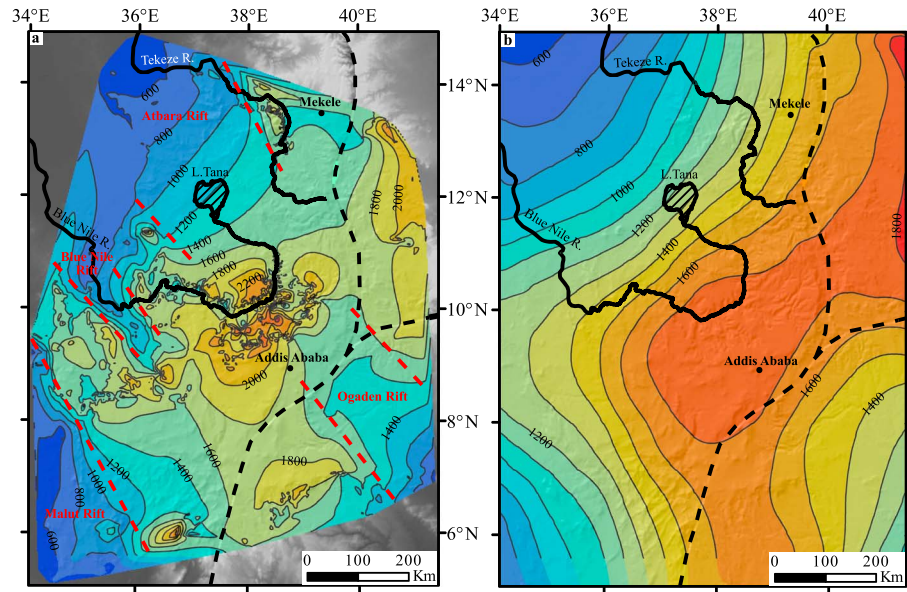


Figure 6. (a) Map of the flood basalt base surface traced on the mosaic DEM (paleogeographic reconstruction of the Oligocene plates configuration based on the palaeotectonic maps of the middle east by *Barrier and Vrielynck [2008]*); the black dashed lines indicate the location of the plates boundaries; the dashed red lines represent the Mesozoic rifts margins (see Figure 3d); (b) post flood basalt topography obtained filtering the flood basalt base surface (Figure 6a) by a circular low-pass filter 200 km in wavelength.

with a maximum elevation of 1000–1100 m. Such features are surrounded by an almost flat landscape with an elevation between 500 and 700 m. The most depressed zones are located immediately east of Addis Ababa and in the northwestern portion of the study area. The locations of such zones mirror the Mesozoic rift basins which characterize the sedimentary basement (Figure 7a).

5. Residual and Dynamic Topography

Further information on the origin of the present topographic signal can be obtained by constructing residual and dynamic topographic maps. After correcting for elastic flexure estimated in the previous section, we obtain the residual topography map by subtracting the inferred isostatic component from the present-day

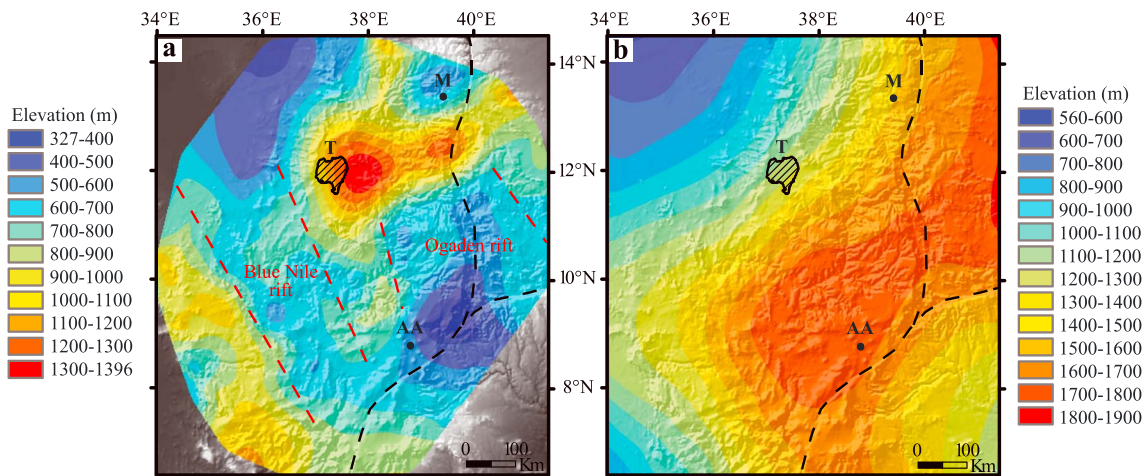


Figure 7. (a) Pre- and (b) post-flood basalt topographies. The black dashed lines indicate the plate boundaries, while the dashed red lines represent the Mesozoic rift margins (see Figure 3d). M = Mekele; AA = Addis Ababa; T = Lake Tana.

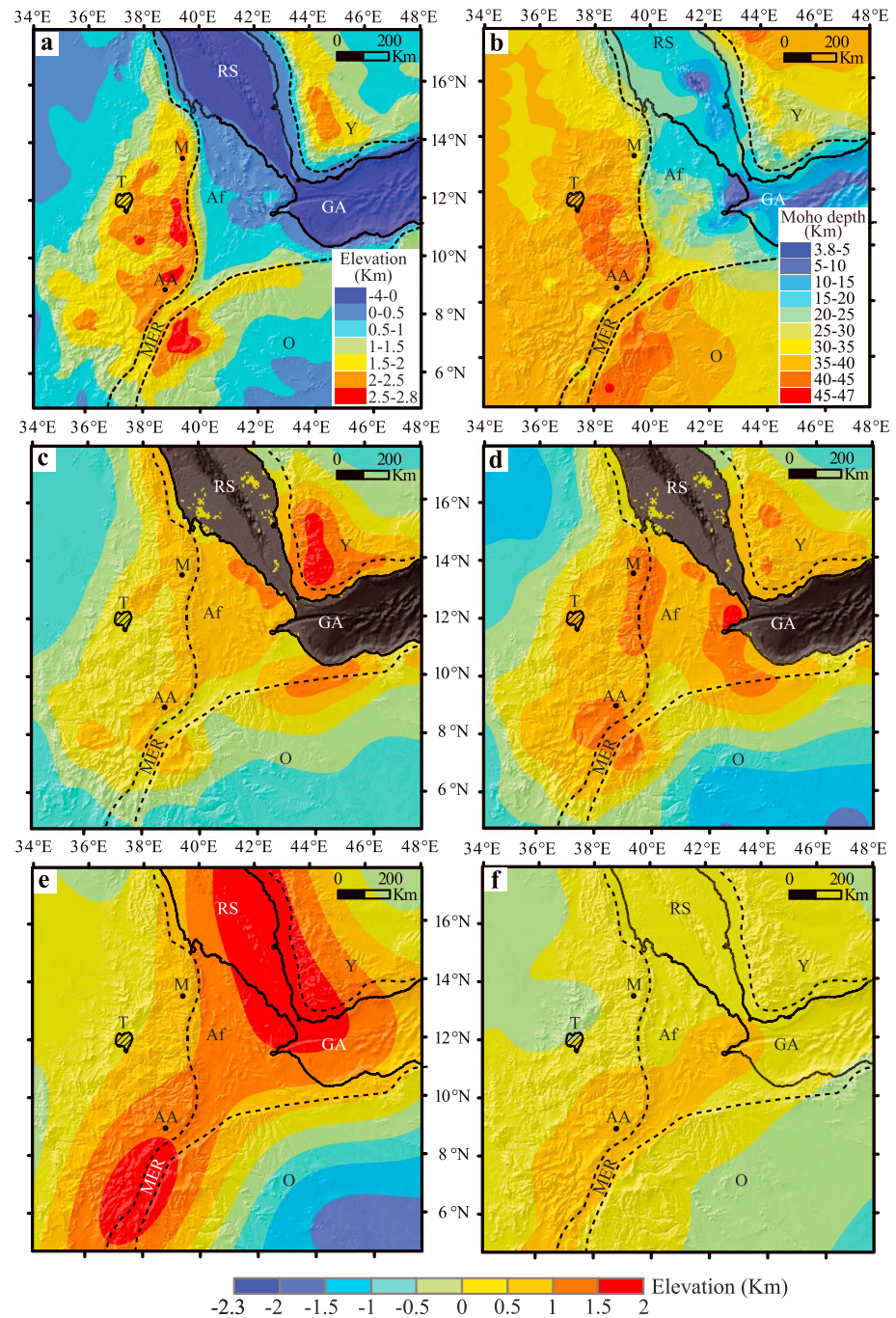


Figure 8. (a) Filtering of the present topography (ETOPO1) by a circular low-pass filter 50 km in wavelength; (b) Moho depth map obtained by merging CRUST1.0 [Laske et al., 2013], Bastow et al. [2008] and Ahmed et al. [2013] Moho depth estimates; (c) non-Airy residual topography (nonflexural actual, observed minus predicted) obtained from CRUST1.0 Moho thickness; (d) residual topography obtained by using the crustal thickness model of Figure 8b, crustal density variations from CRUST1.0, and the lithospheric thickness model of Figure S8; (e) flow-induced dynamic topography for regional wavelengths (spherical harmonic degree, $l > 12$) obtained by merging the upper mantle SL2013 [Schaeffer and Lebedev, 2013] SV model with SAVANI in the lower mantle; (f) flow-induced dynamic topography for regional wavelengths ($l > 12$) resulted from merging the global P wave model LLNL-G3Dv3 [Simmons et al., 2010] with the regional P tomography ETH08 [Bastow et al., 2008]. RS = Red Sea; GA = Gulf of Aden; Af = Afar; Y = Yemen; O = Ogaden.

topography. The result is smoothed with a $6\sigma=300$ km width Gaussian kernel (Figure 8a). The crustal thickness map needed for the Airy isostatic estimate is inferred by considering the available Moho depth constraints for Ethiopia [Mackenzie *et al.*, 2005; Tiberi *et al.*, 2005; Cornwell *et al.*, 2006; Bastow *et al.*, 2008, 2011] and Yemen [Ahmed *et al.*, 2013] (Figure 8b). Such constraints show a change in crustal thickness from ~ 24 km beneath the southern portion of MER to ~ 40 km in the Ethiopian Plateau. In Yemen the crust is ~ 35 km thick decreasing beneath the Red Sea up to ~ 14 km [Mackenzie *et al.*, 2005; Tiberi *et al.*, 2005; Cornwell *et al.*, 2006; Bastow *et al.*, 2008, 2011; Ahmed *et al.*, 2013]. Several studies show high-velocity anomalies in the lower crust both in Ethiopia, interpreted as underplated material at the time of continental flood basalt event [Mackenzie *et al.*, 2005; Stuart *et al.*, 2006; Cornwell *et al.*, 2006; Bastow *et al.*, 2011], and in Yemen, associated to syn-rift mafic intrusions [Ahmed *et al.*, 2013]. The crust and the upper mantle between the location of the Miocene Red Sea rift axis and the current Ethiopian rift axis show high V_p/V_s velocity ratios which have been interpreted as evidence of melt [Kendall *et al.*, 2005; Bastow *et al.*, 2008, 2011; Hammond *et al.*, 2011]. Receiver function studies point out a strong negative phase at depth of ~ 75 – 80 km beneath the rift flank [Rychert *et al.*, 2012]. The absence of this signal beneath the rift has been interpreted as due to decompression melting [Rychert *et al.*, 2012]. Dugda *et al.* [2007] suggest that such structure of the lithosphere can be explained by a plume model, which rapidly thinned the lithosphere by 30–50 km at the time of the flood basalt volcanism, and stacked material beneath the lithosphere.

We compare two models of residual topography of the study area (Figures 8c and 8d). In the first one (Figure 8c) we predict isostatic topography by using a constant crustal and lithospheric density of 2831 kg/m^3 (mean of CRUST 1.0 [Laske *et al.*, 2013]), and 3250 kg/m^3 , respectively, and constant, total lithospheric thickness of 51 km (mean of our lithospheric thickness model, Figure S8). Moho depth is taken from CRUST 1.0 and the asthenospheric density is optimized to minimize the difference between the isostatic topography prediction and the topography reference. The method is standard, with details as in Lachenbruch and Morgan [1990] and Becker *et al.* [2014], for example. In the second model (Figure 8d) the crustal thickness is augmented by the aforementioned regional Moho depth constraints. Lateral crustal density variations are taken from CRUST 1.0 [Laske *et al.*, 2013], and lithospheric thickness variations refer to Figure S8.

The comparison between the two models (Figures 8c and 8d) shows different scenarios. The first model (Figure 8c) shows high positive residual topography values in Yemen and Somalian rift margins (up to 2000 m) and in Afar (up to 1000 m). On the Ethiopian Plateau the model predicts a residual topography of ~ 500 m with local highs close to Addis Ababa and Mekele. The second model presents the highest positive values in Djibouti (up to 1650 m). In Yemen the residual topography (up to 1000 m) is much lower than the one predicted by the first model. Higher positive values are found in the Ethiopian Plateau where we obtain an average residual topography comprised between 750 and 1000 m with peaks of 1500 m in the Mekele and Addis Ababa regions (Figure 8d).

To test if the origin of the topography anomaly may be due to a mantle upwelling [Forte *et al.*, 2010; Moucha and Forte, 2011; Faccenna *et al.*, 2013], we estimate the expected dynamic component of topography (z_{dyn}) induced by convection due to density anomalies in the mantle, as inferred from seismic tomography models (see Figures 8e, 8f, and supporting information). This deflection may be inferred from instantaneous mantle flow related to the radial tractions acting upon a free-slip surface boundary in an incompressible, Newtonian fluid spherical annulus with only radial viscosity variations (for details, see Becker *et al.* [2014]). The density model is constructed by scaling the seismic velocity structure to temperature [Hager *et al.*, 1985; Panasyuk and Hager, 2000]. We also remove the large wavelength (spherical harmonic degree $l < 12$) signatures to emphasize the regional contributions from upper mantle structure. We scale all velocity anomalies below 100 km with a constant velocity to density ratio (no anomalies above 100 km). The tomographic models used are the global, upper mantle SV model SL2013 by Schaeffer and Lebedev [2013], and a merger between the global, multiscale P wave model LLNL-G3Dv3 [Simmons *et al.*, 2010] and the regional tomography ETH08 [Bastow *et al.*, 2008].

Results show positive dynamic topography with a local maximum centered in Addis Ababa with value of up to 1500 m (Figures 8e and 8f), although, as for any such estimates, amplitudes are less well constrained than patterns of anomalies and depend on the tomographic model. Predictions of high dynamic topography are found in a band that is almost parallel to the MER axis (SW-NE trend) elongating from the southern sector of Ethiopia to the Gulf of Aden.

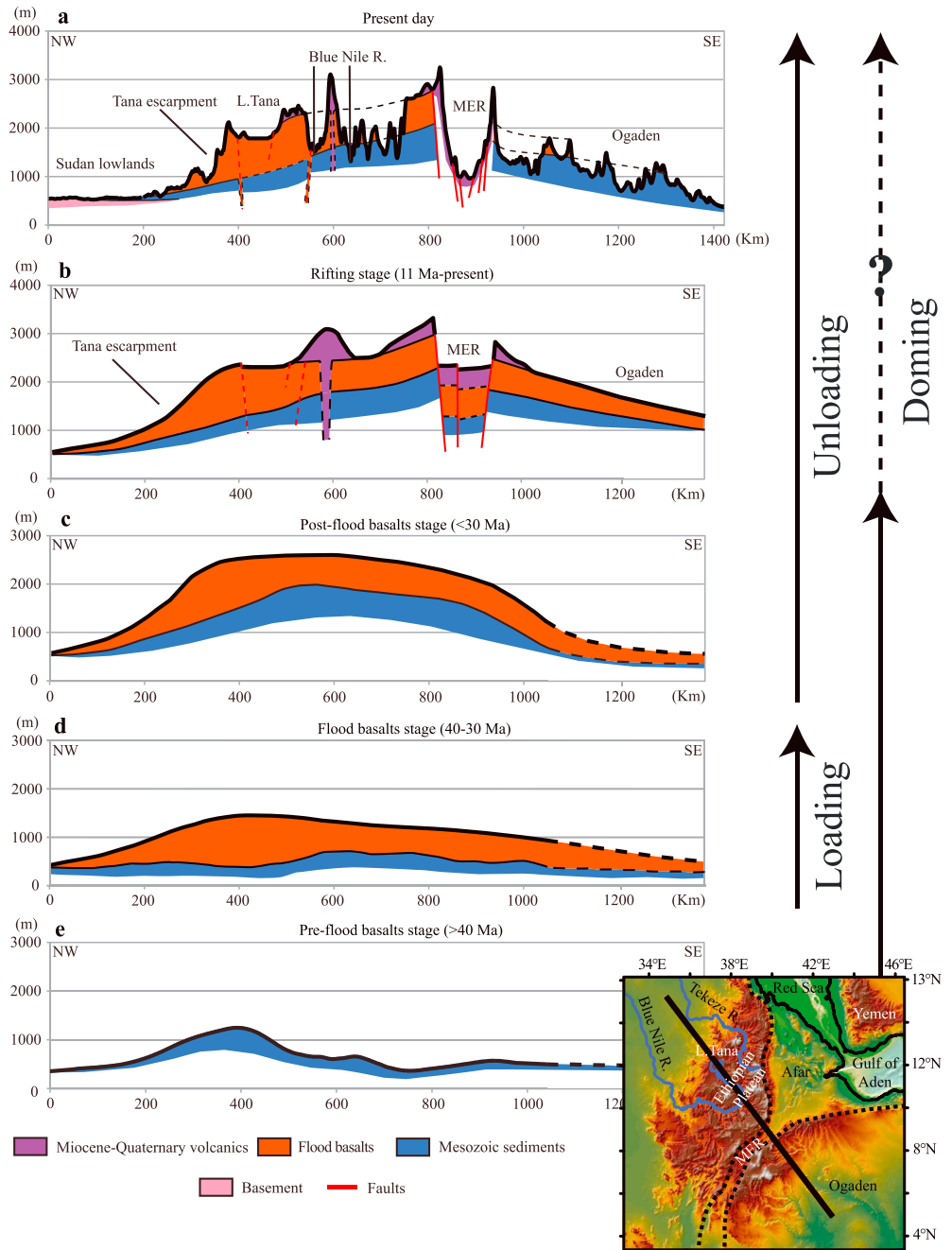


Figure 9. Ethiopian Plateau topographic evolution since pre-Oligocene time, inferred along the cross section of Figure 1a. The extension along the MER, represented in Figure 9a, is based on *Wolfenden et al.* [2004] estimates.

These results indicate that a significant fraction of the present-day, residual topography may be interpreted as dynamically supported by mantle flow. The trend of residual topography indeed mimics the actual topography (see Figures 8a, 8c, and 8d).

6. Discussion

The topographic configuration of the Ethiopian Plateau and surrounding areas is the result of the superimposition of several geologic processes. In the Late Eocene [*Ebinger and Sleep, 1998; Sengör, 2001*] the impinging of hot asthenospheric material at the base of the lithosphere is considered responsible for a large-scale

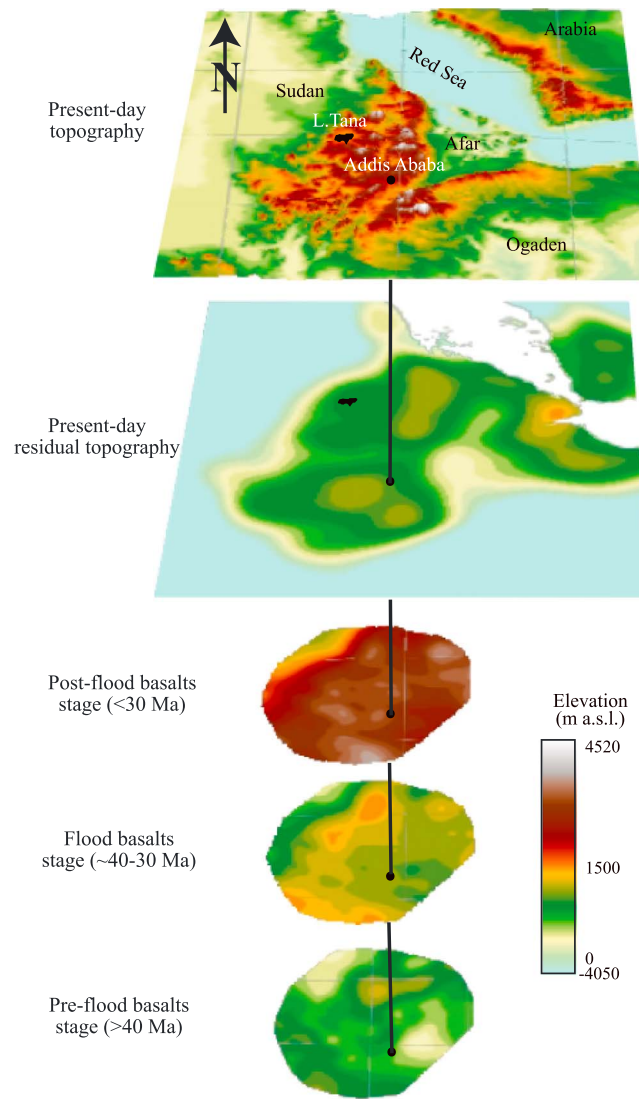


Figure 10. Three-dimensional evolutionary model showing the changes in the topographic configuration of the Ethiopian Plateau and surrounding areas.

doming. Then, in two distinct periods (45 Ma) [Davidson and Rex, 1980; Ebinger et al., 1993; George et al., 1998] and 30–28 Ma [Zumbo et al., 1995; Baker et al., 1996; Hofmann et al., 1997; Rochette et al., 1998], ~900,000 km³ of continental flood basalts were deposited, loading the surface. At the same time, erosion started unloading the surface and flexurally uplifted the western side of the plateau. In the Early Miocene, rifting started in the SW of Ethiopia and in the Turkana region. In the Late Miocene, the northern and central segments of MER formed [Wolfenden et al., 2004; Bonini et al., 2005] causing the flexural uplift of the eastern border of the plateau. Thermochronology and river incision data indicate that uplift occurred after the flood basalt emplacement and on recent times [Pik et al., 2003; Gani et al., 2007].

Our reconstruction, mainly based on the structure and on the geometry of the flood basalts, provides new constraints on the topographic evolution of the region. We may define five main steps along the section of Figure 1a, which crosses the Lake Tana and goes to Ogaden: (1) present-day topography, (2) flexural (un)loading uplift related to rifting, (3) postflood basalt topography prior to rifting, (4) flood basalts stage, and (5) pre-flood basalt topography (Figures 9 and 10).

1. A large fraction of the present-day topographic bulge is dynamically supported by mantle upwellings (Figure 9a). This is in agreement with previous estimates [Daradich et al., 2003; Forte et al., 2010; Moucha and Forte, 2011; Faccenna et al., 2013].
2. In Oligocene time the rifting phase initiated in the Gulf of Aden (30 Ma) [Ahmed et al., 2013] and immediately after in the southern Red Sea (28 Ma) [Wolfenden et al., 2005]. In the Early Miocene the rifting started in the SW Ethiopia and in the Turkana region. The study area has been affected by rifting only in the Late Miocene [Bonini et al., 2005] when the central MER started to form (Figure 9b). The unloading determined by extension along the rift faults (~30 km in the Central MER according to Wolfenden et al. [2004]) caused the flexural uplift along the rift shoulders (Figures 9a and 9b). In addition, erosion of flood basalts on the western side formed and sustained the Tana escarpments. Our best estimate shows that both flexural uplifts extend for some tens to hundreds of kilometers in the inner portion of the plateau (200 km on the rift shoulders and 30 km along the Tana escarpment; see Figures 5a, 5b, and supporting information). The presence of flexural uplift on both eastern and western sides of the plateau (Figure 3b) may be the cause for the formation and conservation of the long standing depression of the Lake Tana (5 Ma according to Mohr [1962]) and of the Ethiopian Plateau. Indeed, the deformation preserved the entire area from erosion inhibiting the capture by the rivers draining Sudan and Afar lowlands. The flexural parameters

that best match the topography range between 1 and 59 km (equivalent elastic thickness, T_e) and between $\sim 5 \cdot 10^{20}$ and $\sim 1 \cdot 10^{24}$ Nm (flexural rigidity D ; see Table S1 in the supporting information). These values are broadly in agreement with previous studies which estimate in the study area an average flexural rigidity of $\sim 10^{23}$ Nm and a lithosphere elastic thickness ranging between 21 and 69 km [Forsyth, 1985; Ebinger et al., 1989; McKenzie and Fairhead, 1997; Pérez-Gussinyé et al., 2009; Tesauro et al., 2012].

The equivalent elastic response of the lithosphere, as shown by the T_e values (see Table S1), depends on the velocity of the unloading event in a viscoelastic lithosphere. In particular, the faster the unloading process the more elastic the response. The tectonic unloading at rift escarpment, caused by the opening of the MER, can be considered a relatively fast event in comparison to the erosional unloading that occurred at the Tana escarpment. Such a difference would be consistent with the difference in values of T_e which are higher in the rift shoulders than along the Tana escarpment (see Table S1).

Also, the crustal thickness plays an important role. According to Burov and Diament [1996], if the crust is thick and sufficiently hot at Moho depths, the upper crust and the uppermost mantle become mechanically decoupled, resulting in a large reduction of effective T_e . Seismological inferences by Benoit et al. [2006] and Bastow et al. [2008, 2011] imply the presence of a large low-velocity anomaly beneath the study area which has been interpreted as rising hot asthenospheric material.

The erosional unloading slightly influenced the topographic configuration of the plateau. Indeed, the maximum flexural uplift is negligible (< 150 m; see Table S3) with respect to the total uplift experienced by the plateau (~ 2000 m) [Pik et al., 2003; Gani et al., 2007]. As the extension kept going the tectonic activity focalized along the rift axis. The volcanic activity, which in the first rifting phase involved large areas along the rift shoulders, was confined in the inner portion of the rift [Ebinger, 2005].

3. After the emplacement of the flood basalts and prior or during the early phase of rifting the entire region was uplifted by a large-wavelength (order of 1000 km) low-amplitude (order of 1 km) bulge (Figure 9c). The axis of the bulge is NNE-SSW oriented following the strike of the Addis Ababa-Mekele ridge and probably extends farther to the southwest and to northeast. The size of the domal uplift is far larger than the one possibly related to crustal processes. We interpret this to mean that the uplift may be related mainly to a dynamic component with contributions coming from deep crustal underplating. This uplift phase is in agreement with what is observed south in Kenya [Wichura et al., 2010]. We cannot exclude that a fraction of this uplift occurred more recently also after the rifting event [Gani et al., 2007].
4. Around 30 Ma [Zumbo et al., 1995; Baker et al., 1996; Hofmann et al., 1997; Rochette et al., 1998] a thick body of basalt quickly flood the entire region (Figure 9d), with an average eruption rate of $1 \text{ km}^3/\text{yr}$ [Rochette et al., 1998]. This enormous volume of basalts caused a subsidence of up to 1140 m (depending on their thickness) and a negligible bulging comprised between 5 and 48 m (see Figure 5c and Table S2). The highest values of subsidence concentrate immediately north of the Lake Tana in correspondence with the Angareb ring complex. This region probably represented one of the main feeding areas of the system [Hahn et al., 1977].
5. Filtering the isostatic and the postflood basalt contributions from the topography, we infer the preflood basalt configuration (Figures 6a and 9e). This surface has an average elevation of ~ 750 m asl and presents two topographic highs in the present Lake Tana region and in the southernmost portion of the study area (Figures 6a and 9e). The lowest values concentrate around Addis Ababa, Mekele, and in the northwestern portion of Ethiopia. Such regions mimic the trend of the Mesozoic rifts developed all over the area such as Blue Nile rift, Atbara rift, and Ogaden rift (see Figures 3d and 6a) [Corti, 2009]. This preflood basalt surface can be referred to the African erosion surface identified all over the continent. Several authors report the presence of a basal unit of red laterite below the Eocene volcanic series in Ethiopia [Merla and Minucci, 1938; Davidson and Rex, 1980; Davidson, 1983], Egypt [Saïd et al., 1976], Yemen [Geukens, 1966; Al-Subbary et al., 1998], and Eritrea [Drury et al., 1994]. The laterite was interpreted as capping a low-relief surface onto which the basalts were emplaced [Burke and Gunnell, 2008].

Most of the preflood basalt surface obtained in the present study lies below 700 m (Figure 6a). Such a value is consistent with Sahagian [1988] and Guiraud and Bosworth [1997] who estimated a mean elevation of ~ 500 m for the whole African continent, stable since the Upper Cretaceous. The relatively high relief sectors (up to 1400 m) in Figure 6a seem to coincide with the Mesozoic rifts shoulders which, according to Sengör [2001]

and Foster and Gleadow [1992, 1996], played an important control on the elevation of the African surface. Indeed, the intracontinental rifts received sedimentary deposits from rivers flowing along the rifts for a long time [Sengör, 2001]. For this reason, there is likely to have been relief on the rift shoulders [Burke and Gunnell, 2008]. Therefore, such sectors could have been subjected to renewed elevation through time (up to 500 m above the average elevation of the African Surface) by erosional unloading [Burke and Gunnell, 2008].

The age of this surface is controversial. By plotting the distribution of marine shorelines, Sengör [2001] showed that the region of northeastern Africa and Arabia was low lying between the beginning of the Paleocene (65 Ma) and late Eocene times (36 Ma). Merla and Minucci [1938] described Ethiopia as having been an area of extremely low relief occupied by a surface of low elevation, product of prevolcanic erosion during Late Cretaceous, Paleocene, and perhaps also Eocene times. The pre-flood basalt surface has been perturbed whenever the upwelling mantle material impinged the base of the East Africa lithosphere forming a dome-shaped topography.

This dome has an average amplitude of a few hundreds of meters. We do not know when this topographic feature formed. The age of the last marine deposit in the area is Upper Jurassic [Bosellini et al., 1995]. However, based on the shape and wavelength and its relationships with basalt source, we may reasonably assume that also this domal uplift can be related to a mantle upwelling. Our reconstruction also points out the presence of smaller wavelength features. This may well be ascribed to crustal underplating [Mackenzie et al., 2005].

Assessing the evolution of the region, we note that the large scale pre-flood, post-flood basalts and present residual and dynamic topographies all show similar topographic anomalies (Figures 7a, 7b, 8c, and 8f). This suggests that the topographic pattern remained almost unchanged over a long period of time, as inferred from thermochronological data [Pik et al., 2003]. The center of the topography anomaly is indeed located in the proximities of the low seismic velocity shown in the *P* and *S* waves velocity [Benoit et al., 2006; Bastow et al., 2008, 2011; Hammond et al., 2010; Nyblade, 2011; Hansen and Nyblade, 2013].

Unfortunately, we do not have data to establish if the Ethiopian Plateau is still uplifting today. However, from comparison between residual and dynamic topography it is probable that mantle flow supports the elevation of the plateau at present. If this model is correct, we should then expect a source of mantle upwelling that is sustained for a period of almost 30–40 Ma, inducing uplift of more than ~1500 m over a period of time of ~35 Ma, resulting in an average uplift velocity of ~0.04 mm/yr. Of course, this is a minimum estimate and most likely the uplift could have been discontinuous resulting on higher rate pulse of uplift. Lastly, this reconstruction reconciles previous suggestions of a long-term uplift of the plateau [Pik et al., 2003] and dynamic topography models suggesting a continuous swell underneath the region of ~1000 m during the last ~30 Ma [Moucha and Forte, 2011]. If the model of a long-term supported dome is correct, we would then infer a rather stationary mantle upwelling history, perhaps associated with an increase in upwelling velocity. It is expressed, first, by an initial ~800 m high, small dome (~35–45 Ma), then generates flood basalts and keeps producing volcanism, arching, and doming, and eventually leading to continental rifting during the separation of Arabia and Somalia from Africa. Our data may be used to constrain mantle upwelling models and their complex interaction with the lithosphere [Burov and Guillou-Frottier, 2005; Burov et al., 2007; Moucha and Forte, 2011; Burov and Gerya, 2014].

7. Conclusions

We use the geometry of the flood basalt event in Ethiopia to reconstruct the topographic evolution of the area. We then compare the paleotopography evolution with present-day residual and dynamic topography. The results can be summarized as follows:

1. Flood basalts form a large-scale dome, asymmetrical with respect to the Afar depression and to the rift valley, with maximum thickness around Lake Tana.
2. The flexural uplift along the Ethiopian Plateau escarpments extends for some tens to hundreds of kilometers in the inner portion of the plateau (200 km on the rift shoulders and 30 km along the Tana escarpment). The presence of flexural uplift on both eastern and western sides of the plateau probably determined the formation and conservation of the Ethiopian Plateau and of the Lake Tana depression. Indeed, the flexural deformation inhibited the capture of the plateau internal drainage by the rivers draining Sudan and Afar lowlands. The load of basalts caused subsidence ranging between ~100 and ~1100 m, and bulging comprised between 5 and ~50 m.

3. After the emplacement of the flood basalts, the entire region was uplifted, forming a large-scale dome with an NNE trending axis, producing an uplift of more than ~1000 m along its crest line.
4. Flood basalts were emplaced over a hilly region around 30 Ma, with two preexisting topographic highs corresponding to the area between Addis Ababa and Mekele (maximum elevation of ~1300–1400 m) and to the southwestern portion of the study area (maximum elevation of 1000–1100 m). Such surfaces can be referred to the African erosion surface identified all over the continent.
5. The positive residual topography bulge ranges between 500 and 1000 m and presents two peaks centered in the Addis Ababa and Mekele areas. Such peaks appear to broadly align with inferred dynamic topography anomalies. This suggests that a fraction of the present-day topography is dynamically supported by mantle upwelling.

In conclusion, the pre-flood and post-flood basalt reconstructions show similar topographic features. Those features resemble the ones observed in the residual and dynamic topography analysis. This suggests that the topographic pattern all over the area remained almost unchanged over a long period of time with the center of the topography anomaly (~1500 m) located in the proximities of the shallow low-seismic velocity. If this model is correct, we expect a source of mantle upwelling inducing an average uplift of more than ~1500 m over ~35 Ma. We conclude that the growth of the Ethiopian Plateau is a long-term, probably still active, dynamically-supported process.

Acknowledgments

Discussion with Francesco Salvini, Sean Willett, and Emanuele Giachetta were helpful during the preparation of this manuscript. We thank Cindy Ebinger and Ernesto Abbate for their comments that greatly improved the manuscript. Supporting information data are included in an SI file; any additional data may be obtained from the corresponding author (email: andrea.sembroni@uniroma3.it).

References

- Abbate, E., P. Bruni, and M. Sagri (2015), Geology of Ethiopia: A review and geomorphological perspectives, in *Landscapes and Landforms of Ethiopia, World Geomorphological Landscapes*, edited by P. Billi, Springer Science + Business Media, Dordrecht, doi:10.1007/978-94-017-8026-1_2.
- Ahmed, A., C. Tiberi, S. Leroy, G. W. Stuart, D. Keir, J. Sholan, K. Khanbari, I. Al-Ganad, and C. Basuyau (2013), Crustal structure of the rifted volcanic margins and uplifted plateau of Western Yemen from receiver function analysis, *Geophys. J. Int.*, *193*(3), 1673–1690.
- Al-Subary, A. K., G. N. Nichols, D. W. J. Bosence, and M. Al-Kadasi (1998), Pre-rift forming, peneplanation or subsidence in the southern Red Sea? Evidence from the Medj-zir Formation (Tawilah Group) of western Yemen, in *Sedimentation and Tectonics in Rift Basins: Red Sea-Gulf of Aden Case*, edited by B. Purser and D. Bosence, pp. 119–134, Chapman and Hall, London.
- As-Saruri, M. (2004), Geological map of Yemen, Ministry of oil and minerals petroleum exploration and production authority.
- Baker, B. H., P. A. Mohr, and L. A. J. Williams (1972), Geology of the Eastern Rift System of Africa, *Geol. Soc. Am. Spec. Pap.*, *136*, 1–67.
- Baker, J., L. Snee, and M. Menzies (1996), A brief Oligocene period of flood volcanism in Yemen, *Earth Planet. Sci. Lett.*, *138*, 39–55.
- Barrier, E., and B. Vrielynck (2008), Paleotectonic maps of the Middle East: Atlas of 14 maps, Middle East Basin Evolution (MEBE) Programme.
- Bastow, I. D., A. A. Nyblade, G. W. Stuart, T. O. Rooney, and M. H. Benoit (2008), Upper mantle seismic structure beneath the Ethiopian hot spot: Rifting at the edge of the African low-velocity anomaly, *Geochem. Geophys. Geosyst.*, *9*, Q12022, doi:10.1029/2008GC002107.
- Bastow, I. D., D. Keir, and E. Daly (2011), The Ethiopia Afar Geoscientific Lithospheric Experiment (EAGLE): Probing the transition from continental rifting to incipient sea floor spreading, *Geol. Soc. Am., Soc. Pap.*, vol. 478, ISSN: 1366-8781.
- Becker, T. W., C. Faccenna, E. D. Humphreys, A. R. Lowry, and M. S. Miller (2014), Static and dynamic support of western U.S. topography, *Earth Planet. Sci. Lett.*, *402*, 234–246.
- Benoit, M. H., A. A. Nyblade, and J. C. VanDecar (2006), Upper mantle *P* wave speed variations beneath Ethiopia and the origin of the Afar Hotspot, *Geology*, *34*, 329–332.
- Berhe, S. M., B. Desta, M. Nicoletti, and M. Tefera (1987), Geology, geochronology and geodynamic implications of the Cenozoic magmatic province in W and SE Ethiopia, *J. Geol. Soc. London*, *144*, 213–226.
- Beydoun, Z. R. (1960), Synopsis of the geology of East Aden Protectorate, XXI Int. Geol. Congress, Copenhagen 21, pp. 131–149.
- Bonini, M., G. Corti, F. Innocenti, P. Manetti, F. Mazzarini, T. Abebe, and Z. Pecskey (2005), Evolution of the Main Ethiopian Rift in the frame of Afar and Kenya rifts propagation, *Tectonics*, *24*, TC1007, doi:10.1029/2004TC001680.
- Boschi, C., C. Faccenna, and T. W. Becker (2010), Mantle structure and dynamic topography in the Mediterranean basin, *Geophys. Res. Lett.*, *37*, L20303, doi:10.1029/2010GL045001.
- Bosellini, A., A. Russo, and G. Assefa (1995), Il Calcare di Antalo nella regione di Macallè (Tigray, Etiopia settentrionale), *Rend. Fis. Acc. Lincei*, *6*, 253–267.
- Bosworth, W., P. Huchon, and K. McClay (2005), The Red Sea and Gulf of Aden Basins, *J. Afr. Earth Sci.*, *43*, 334–378.
- Braun, J. (2010), The many surface expressions of mantle dynamic, *Nat. Geosci.*, *3*, 825–833.
- Braun, J., X. Robert, and T. Simon-Labric (2013), Eroding dynamic topography, *Geophys. Res. Lett.*, *40*, 1494–1499, doi:10.1002/grl.50310.
- Burbank, D. W., and R. S. Anderson (2011), *Tectonic Geomorphology*, 2nd ed., Wiley-Blackwell, Oxford, U. K.
- Burke, K. (1996), The African plate, *S. Afr. J. Geol.*, *99*, 339–409.
- Burke, K., and Y. Gunnell (2008), The African erosion surface: A continental-scale synthesis of geomorphology, tectonics, and environmental change over the past 180 million years, *Geol. Soc. Am. Mem.*, *201*, 1–66.
- Burov, E., and M. Diament (1996), Isostasy, equivalent elastic thickness, and inelastic rheology of continents and oceans, *Geology*, *24*(5), 419–422.
- Burov, E., and T. Gerya (2014), Asymmetric three-dimensional topography over mantle plumes, *Nature*, *513*, 85–89.
- Burov, E., and L. Guillou-Frottier (2005), The plume-head continental lithosphere interaction using a tectonically realistic formulation for the lithosphere, *Geophys. J. Int.*, *58*, doi:10.1111/j.136-246x.2005.02588.x.
- Burov, E., L. Guillou-Frottier, E. D'acremont, L. Le Pourhiet, and S. Cloetingh (2007), Plume head–lithosphere interactions near intra-continental plate boundaries, *Tectonophysics*, *434*(1), 15–38, doi:10.1016/j.tecto.2007.01.002.
- Chorowicz, J., B. Collet, F. F. Bonavia, P. Mohr, J.-F. Parrot, and T. Korme (1998), The Tana basin, Ethiopia: Intra plateau uplift, rifting and subsidenc, *Tectonophysics*, *295*, 351–367.

- Chumburo, F. (2009), Geological map of DebreMarkos sheet (NC 37-6), EIGS.
- Cornwell, D. G., G. D. McKenzie, P. K. H. Maguire, R. W. England, L. M. Asfaw, and B. Oluma (2006), Northern Main Ethiopian Rift crustal structure from new high-precision gravity data, *Geol. Soc. London, Spec. Publ.*, 259, 307–321, doi:10.1144/GSL.SP.2006.259.01.23.
- Cornwell, D. G., P. K. H. Maguire, R. W. England, and G. W. Stuart (2010), Imaging detailed crustal structure and magmatic intrusion across the Ethiopian Rift using a dense linear broadband array, *Geochem. Geophys. Geosyst.*, 11, Q0AB03, doi:10.1029/2009GC002637.
- Corti, G. (2009), Continental rift evolution: From rift initiation to incipient break-up in the Main Ethiopian Rift, East Africa, *Earth Sci. Rev.*, 96, 1–53.
- Courtilot, V., C. Jaupart, I. Manighetti, P. Tapponnier, and J. Besse (1999), On causal links between flood basalts and continental breakup, *Earth Planet. Sci. Lett.*, 166, 177–195.
- D'Agostino, N., and D. P. McKenzie (1999), Convective support of long wavelength topography in the Apennines (Italy), *Terra Nova*, 11, 234–238.
- Dainelli, G. (1943), *Geologia dell'Africa Orientale* (3 vols. text, 1 vol. maps), *R. Accad. Ital.*, Roma.
- Daradich, A., J. X. Mitrovica, R. N. Pysklywec, S. D. Willett, and A. M. Forte (2003), Mantle flow, dynamic topography, and rift-flank uplift of Arabia, *Geology*, 31, 901–904.
- Davidson, A. (1983), The Omo River project: Reconnaissance geology and geochemistry of parts of Ilubabor, Kefa, Gemu Gofa, and Sidamo, *Ethiopian Institute of Geological Surveys, Bulletin* 2, 89 p.
- Davidson, A., and D. C. Rex (1980), Age of volcanism and rifting in south-western Ethiopia, *Nature*, 283, 654–658.
- Drury, S. A., S. P. Kelley, S. M. Berhe, R. E. L. I. Collier, and M. Abraha (1994), Structures related to Red Sea evolution in northern Eritrea, *Tectonics*, 13, 1371–1380, doi:10.1029/94TC01990.
- Dugda, M. T., A. A. Nyblade, and J. Julià (2007), Thin lithosphere beneath Ethiopia and Djibouti revealed by a joint inversion of Rayleigh wave group velocities and receiver functions, *J. Geophys. Res.*, 112, B08305, doi:10.1029/2006JB004918.
- Ebinger, C. (2005), Continental breakup: The East African perspective, *Astron. Geophys.*, 46, 2.16–2.21.
- Ebinger, C., and N. H. Sleep (1998), Cenozoic magmatism in central and east Africa resulting from impact of one large plume, *Nature*, 395, 788–791.
- Ebinger, C. J., and M. Casey (2001), Continental breakup in magmatic provinces: An Ethiopian example, *Geology*, 29, 527–530.
- Ebinger, C. J., and N. J. Hayward (1996), Soft plates and hot spots: Views from Afar, *J. Geophys. Res.*, 101, 21,859–21,876, doi:10.1029/96JB02118.
- Ebinger, C. J., T. D. Bechtel, D. W. Forsyth, and C. O. Bowin (1989), Effective elastic thickness beneath the East African and Afar plateaus and dynamic compensation for the uplifts, *J. Geophys. Res.*, 94, 2883–2901, doi:10.1029/JB094iB03p02883.
- Ebinger, C. J., T. Yemane, G. WoldeGabriel, J. L. Aronson, and R. C. Walter (1993), Late Eocene—Recent volcanism and faulting in the southern main Ethiopian rift, *J. Geol. Soc. London*, 150, 99–108.
- Faccenna, C., P. Molin, B. Orecchio, V. Olivetti, O. Bellier, F. Funicello, L. Minelli, C. Piromallo, and A. Billi (2011), Topography of the Calabria subduction zone (southern Italy): Clues for the origin of Mt. Etna, *Tectonics*, 30, TC1003, doi:10.1029/2010TC002694.
- Faccenna, C., T. W. Becker, L. Jolivet, and M. Keskin (2013), Mantle convection in the Middle East: Reconciling Afar upwelling, Arabia indentation and Aegean trench rollback, *Earth Planet. Sci. Lett.*, 375, 254–269.
- Forsyth, D. W. (1985), Subsurface loading and estimates of the flexural rigidity of continental lithosphere, *J. Geophys. Res.*, 90(B14), 12,623–12,632, doi:10.1029/JB090iB14p12623.
- Forte, A. M., S. Quere, R. Moucha, N. A. Simmons, S. P. Grand, J. X. Mitrovica, and D. B. Rowley (2010), Joint seismic-geodynamic-mineral physical modelling of African geodynamics: A reconciliation of deep-mantle convection with surface geophysical constraints, *Earth Planet. Sci. Lett.*, doi:10.1016/j.epsl.2010.03.017.
- Foster, D. A., and A. J. W. Gladow (1992), The morphotectonic evolution of rift-margin mountains in Central Kenya: Constraints from apatite fission track thermochronology, *Earth Planet. Sci. Lett.*, 113, 157–171, doi:10.1016/0012-821X(92)90217-J.
- Foster, D. A., and A. J. W. Gladow (1996), Structural framework and denudation history of the flank of the Kenya and Anza Rifts, East Africa, *Tectonics*, 15, 258–271, doi:10.1029/95TC02744.
- Furman, T., J. Bryce, T. Rooney, B. Hanan, G. Yurgu, and D. Ayalew (2006), Heads and tails: 30 million years of the Afar plume, *Geol. Soc. Am. Spec. Publ.*, 259, 95–119, doi:10.1144/GSL.SP.2006.259.01.09.
- Geological and Mineral Resources Department (1981), Geological map of the Sudan, Geological and mineral resources department.
- Gani, N. D., M. G. Abdelsalam, and M. R. Gani (2007), Blue Nile incision on the Ethiopian Plateau: Pulsed plateau growth, Pliocene uplift, and hominin evolution, *Geol. Soc. Am. Today*, 17, 4–11.
- Gani, N. D. S., M. G. Abdelsalam, S. Gera, and M. R. Gani (2008), Stratigraphic and structural evolution of the Blue Nile Basin, Northwestern Ethiopian Plateau, *Geol. J.*, 44, 30–56.
- Garland, C. R. (1980), *Geology of the Adigrat Area, Memoir* 1, 51 pp., Ministry of Mines, Addis Ababa.
- George, R., N. Rogers, and S. Kelley (1998), Earliest magmatism in Ethiopia: Evidence for two mantle plumes in one flood basalts province, *Geology*, 26, 923–926.
- Geukens, F. (1966), Geology of the Arabian Peninsula: Yemen, *U.S. Geol. Surv. Prof. Pap.*, 560-B, p. 23.
- Guiraud, R., and W. Bosworth (1997), Senonian basin inversion and rejuvenation of rifting in Africa and Arabia: Synthesis and application to plate-scale tectonics, *Tectonophysics*, 282, 39–82, doi:10.1016/S0040-1951(97)00212-6.
- Guiraud, R., W. Bosworth, J. Thierry, and A. Delplanque (2005), Phanerozoic geological evolution of Northern and Central Africa: An overview, *J. Afr. Earth Sci.*, 43, 83–143, doi:10.1016/j.jafrearsci.2005.07.017.
- Gurnis, M. (2001), Sculpting the Earth from inside out, *Sci. Am.*, 284, 40–47.
- Gurnis, M., J. X. Mitrovica, J. Ritsema, and H. J. van Heijst (2000), Constraining mantle density structure using geological evidence of surface uplift rates: The case of the African Superplume, *Geochem. Geophys. Geosyst.*, 1, 1020, doi:10.1029/1999GC000035.
- Hager, B. H., R. W. Clayton, M. A. Richards, R. P. Comer, and A. M. Dziewonski (1985), Lower mantle heterogeneity, dynamic topography and the geoid, *Nature*, 313, 541–545.
- Hagos, M., C. Koeberl, K. Kabeto, and F. Koller (2010), Geochemical characteristics of the alkaline basalt and the phonolite–trachyte plugs of the Axum area, northern Ethiopia, *Aust. J. Earth Sci.*, 103(2), 153–170.
- Hahn, G. A., R. G. H. Reynolds, and R. A. Wood (1977), The geology of the Angareb Ring Dike complex, northwestern Ethiopia, *Bull. Volcanol.*, 40, 1–10.
- Hailu, T. (1975), Geological Map of Adiarkay Sheet (ND 37-10), 1:250,000, EIGS.
- Hammond, J. O. S., J.-M. Kendall, D. Angus, and J. Wookey (2010), Interpreting spatial variations in anisotropy: Insights into the Main Ethiopian Rift from SKS waveform modeling, *Geophys. J. Int.*, 181, 1701–1712.
- Hammond, J. O. S., J.-M. Kendall, G. W. Stuart, D. Keir, C. J. Ebinger, A. Ayele, and M. Belachew (2011), The nature of the crust beneath the Afar triple junction: Evidence from receiver functions, *Geochem. Geophys. Geosyst.*, 12, Q12004, doi:10.1029/2011GC003738.

- Hansen, S. E., and A. A. Nyblade (2013), The deep seismic structure of the Ethiopia/Afar hotspot and the African superplume, *Geophys. J. Int.*, doi:10.1093/gji/ggt116.
- Hautot, S., K. Whaler, W. Gebru, and M. Desissa (2006), The structure of a Mesozoic basin beneath the Lake Tana area, Ethiopia, revealed by magnetotelluric imaging, *J. Afr. Earth Sci.*, *44*, 331–338.
- Hofmann, C., V. Courtillot, G. Feraud, P. Rochette, G. Yirgu, E. Ketefo, and R. Pik (1997), Timing of the Ethiopian flood basalt event and implications for plume birth and global change, *Nature*, *389*, 838–841.
- Jepsen, D. H., and M. J. Athearn (1961), A general geological map of the Blue Nile River basin, Ethiopia (1:1,000,000), *Dep. Water Resources*, Addis Ababa.
- Kazmin, V. (1976), Geological Map of Adigrat Sheet (ND 37-7), 1:250,000, *EIGS*.
- Kebede, S. (2013), *Groundwater in Ethiopia—Features, Numbers and Opportunities*, Springer, Berlin.
- Kendall, J. M., G. W. Stuart, C. J. Ebinger, I. D. Bastow, and D. Keir (2005), Magma assisted rifting in Ethiopia, *Nature*, *433*, 146–148.
- Kieffer, B., et al. (2004), Flood and shield basalt from Ethiopia: Magmas from the African Superswell, *J. Petrol.*, *45*, 793–834, doi:10.1093/ptrology/egg112.
- Lachenbruch, A. H., and P. Morgan (1990), Continental extension, magmatism and elevation; formal relations and rules of thumb, *Tectonophysics*, *174*, 39–62.
- Laske, G., G. Masters, Z. Ma, and M. Pasyanos (2013), Update on CRUST1.0—A 1-degree global model of Earth's crust, *Geophys. Res. Abstracts*, *15*, Abstract EGU2013-2658.
- Lithgow-Bertelloni, C., and P. G. Silver (1998), Dynamic topography, plate driving forces and the African superswell, *Nature*, *395*, 269–272, doi:10.1038/26212.
- Mackenzie, G. H., H. Thybo, and P. Maguire (2005), Crustal velocity structure across the Main Ethiopian Rift: Results from two-dimensional wide-angle seismic modelling, *Geophys. J. Int.*, *162*, 994–1006.
- Mattash, M. A., L. Pinarelli, O. Vaselli, A. Minissale, M. Al-Kadasi, M. N. Shawki, and F. Tassi (2013), Continental flood basalts and rifting: Geochemistry of Cenozoic Yemen volcanic province, *Int. J. Geosci.*, *4*, 1459–1466.
- McDougall, I., W. H. Morton, and M. A. J. William (1975), Ages and rates of denudation of Trap Series basalt at the Blue Nile Gorge, Ethiopia, *Nature*, *254*, 207–209.
- McKenzie, D., and D. Fairhead (1997), Estimates of the effective elastic thickness of the continental lithosphere from Bouger and free air gravity anomalies, *J. Geophys. Res.*, *102*, 27,523–27,552, doi:10.1029/97JB02481.
- Mege, D., and T. Korme (2004), Dyke swarm emplacement in the Ethiopian Large Igneous Province: Not only a matter of stress, *J. Volcanol. Geotherm. Res.*, *132*, 283–310.
- Merla, G., and E. Minucci (1938), *Missione geologica nel Tigre*, Volume 1, La serie dei terreni, Rome, Reale Accademia d'Italia, Centro Studi per l'Africa Orientale Italiana, vol. 3, 363 p.
- Merla, G., E. Abbate, P. Canuti, M. Sagri, and P. Tacconi (1979), Geological map of Ethiopia and Somalia and comment with a map of major landforms (scale 1:2,000,000), CNR, Rome. 95.
- Minucci, E. (1938), Ricerche geologiche nella regione del Tana, in *Missione di Studio al Lago Tana*, vol. 1, pp. 19–36, R. Accad. Ital., Roma.
- Mohr, P., and B. Zanettin (1988), The Ethiopian flood basalts province, in *Continental Flood basalts*, edited by J. D. McDougall, pp. 63–110, Kluwer Acad., Dordrecht, Netherlands.
- Mohr, P. A. (1962), *The Geology of Ethiopia*, Addis Ababa Univ. Press, Addis Ababa.
- Mohr, P. A. (1967), The Ethiopian Rift System, *Bull. Geophys. Obs. Addis Ababa*, *11*, 1–65.
- Mohr, P. A. (1983), Ethiopian flood basalts province, *Nature*, *303*, 577–584, doi:10.1038/303577a0.
- Molin, P., F. J. Pazzaglia, and F. Dramis (2004), Geomorphic expression of active tectonics in a rapidly deforming forearc, Sila Massif, Calabria, southern Italy, *Am. J. Sci.*, *304*, 559–589.
- Molin, P., G. Fubelli, M. Nocentini, S. Sperini, P. Ignat, F. Grecu, and F. Dramis (2011), Interaction of mantle dynamics, crustal tectonics and surface processes in the topography of the Romanian Carpathians: A geomorphological approach, *Global Planet. Change*, doi:10.1016/j.gloplacha.2011.05.005.
- Molnar, P., and P. England (1990), Late Cenozoic uplift of mountain ranges and global climate change: Chicken or egg?, *Nature*, *346*, 29–34.
- Moucha, R., and A. M. Forte (2011), Changes in African topography driven by mantle convection, *Nat. Geosci. Lett.*, doi:10.1038/NGEO1235.
- Moucha, R., A. M. Forte, J. X. Mitrovica, D. B. Rowley, S. Quere, N. A. Simmons, and S. P. Grand (2008), Dynamic topography and long-term sea-level variations: There is no such thing as a stable continental platform, *Earth Planet. Sci. Lett.*, *271*, 101–108, doi:10.1016/j.epsl.2008.03.056.
- Natali, C., L. Beccaluva, G. Bianchini, and F. Siena (2013), The Axum-Adwa basalt-trachyte complex: A late magmatic activity at the periphery of the Afar plume, *Contrib. Mineral. Petrol.*, *166*, 351–370.
- Nyblade, A. A. (2011), The upper-mantle low-velocity anomaly beneath Ethiopia, Kenya, and Tanzania: Constraints on the origin of the African superswell in eastern Africa and plate versus plume models of mantle dynamics, *Geol. Soc. Am. Spec. Pap.*, *478*, 37–50.
- Nyblade, A. A., and C. A. Langston (2002), Broadband seismic experiments probe the East African rift, *EOS Trans. AGU*, *83*, 405–408.
- Panasjuk, S. V., and B. H. Hager (2000), Models of isostatic and dynamic topography, geoid anomalies, and their uncertainties, *J. Geophys. Res.*, *105*, 28,199–28,209, doi:10.1029/2000JB900249.
- Pérez-Gussinyé, M., J. P. Morgan, T. J. Reston, and C. R. Ranero (2006), From rifting to spreading at non-volcanic margins: Insights from numerical modeling, *Earth Planet. Sci. Lett.*, *244*, 458–473.
- Pérez-Gussinyé, M., M. Metois, M. Fernández, J. Vergés, J. Fulla, and A. R. Lowry (2009), Effective elastic thickness of Africa and its relationship to other proxies for lithospheric structure and surface tectonics, *Earth Planet. Sci. Lett.*, *287*, 152–167, doi:10.1026/j.epsl.2009.08.004.
- Pik, R., C. Deniel, C. Coulon, G. Yirgu, and B. Marty (1999), Isotopic and trace element signatures of Ethiopian basalts: Evidence for plume-lithospheric interactions, *Geochim. Cosmochim. Acta*, *63*, 2263–2279.
- Pik, R., B. Marty, J. Carignan, and J. Lave (2003), Stability of Upper Nile drainage network (Ethiopia) deduces from (U–Th)/He thermochronometry: Implication of uplift and erosion of the Afar plume dome, *Earth Planet. Sci. Lett.*, *215*, 73–88, doi:10.1016/S0012-821X(03)00457-6.
- Ritsema, J., H. J. van Heijst, and J. H. Woodhouse (1999), Complex shear wave velocity structure imaged beneath Africa and Iceland, *Science*, *286*, 1925–1928, doi:10.1126/science.286.5446.1925.
- Rochette, P., E. Tamrat, G. Feraud, R. Pik, V. Courtillot, E. Ketefo, C. Coulon, C. Hoffmann, D. Vandamme, and G. Yirgu (1998), Magnetostratigraphy and timing of the Oligocene Ethiopian Traps, *Earth Planet. Sci. Lett.*, *164*, 497–510.
- Rogers, N., R. Macdonald, J. Fitton, R. George, R. Smith, and B. Barreiro (2000), Two mantle plumes beneath the East African rift system: Sr, Nd and Pb isotope evidence from Kenya Rift basalt, *Earth Planet. Sci. Lett.*, *176*, 387–400.

- Rogers, N. W. (2006), Basaltic magmatism and the geodynamics of the East African Rift System, *Geol. Soc. Spec. Publ.*, 259, 77–93, doi:10.1144/GSL.SP.2006.259.01.08.
- Roy, M., T. H. Jordan, and J. Pederson (2009), Colorado Plateau magmatism and uplift by warming of heterogeneous lithosphere, *Nature*, 459, 978–982.
- Rychert, C. A., J. O. S. Hammond, N. Harmon, J. M. Kendall, D. Keir, C. J. Ebinger, I. D. Bastow, A. Ayele, M. Belachew, and G. Stuart (2012), Volcanism in the Afar Rift sustained by decompression melting with minimal plume influence, *Nat. Geosci.*, 5, 406–409.
- Sahagian, D. L. (1988), Epeirogenic motion of Africa as inferred from Cretaceous shoreline deposits, *Tectonics*, 7, 125–138, doi:10.1029/TC007i001p00125.
- Said, R., A. H. Sabet, A. A. Zalata, V. A. Teniakov, and V. I. Pokryshkin (1976), A review of theories of the geological distribution of bauxite and their application for bauxite prospecting in Egypt, *Ann. Geol. Surv. Egypt*, 6, 6–31.
- Schaeffer, A., and J. S. Lebedev (2013), Global shear-speed structure of the upper mantle and transition zone, *Geophys. J. Int.*, 194, 417–449.
- Schilling, J. G., R. H. Kingsley, B. B. Hanan, and B. L. McCully (1992), Nd-Sr-Pb isotopic variations along the Gulf of Aden: Evidence for Afar mantle plume-continental lithosphere interaction, *J. Geophys. Res.*, 97(B7), 10, 927–10,966, doi:10.1029/92JB00415.
- Sengör, A. M. C. (2001), Elevation as indicator of mantle-plume activity, *Geol. Soc. Am., Spec. Pap.*, 352, 183–225.
- Sepulchre, P., G. Ramstein, F. Fluteau, M. Schuster, J. J. Tiercelin, and M. Brunet (2006), Tectonic uplift and eastern Africa aridification, *Science*, 313, 1419–1423.
- Simmons, N. A., A. M. Forte, L. Boschi, and S. P. Grand (2010), GyPSuM: A joint tomographic model of mantle density and seismic wave speeds, *J. Geophys. Res.*, 115, B12310, doi:10.1029/2010JB007631.
- Stern, R. J. (1994), Arc assembly and continental collision in the Neoproterozoic East African orogen, *Annu. Rev. Earth Planet. Sci.*, 22, 319–351.
- Stuart, G. W., I. D. Bastow, and C. J. Ebinger (2006), Crustal structure of the northern Main Ethiopian Rift from receiver function studies, *Geol. Soc. Spec. Publ.*, 259, 253–267.
- Tefera, M., T. Cherenet, and W. Haro (1996), Geological map of Ethiopia (1:2,000,000), *Ethiopian Institute of Geological Survey*, Addis Ababa, Ethiopia.
- Tesaro, M., P. Audet, M. K. Kaban, R. Burgmann, and S. Cloetingh (2012), The effective elastic thickness of the continental lithosphere: Comparison between rheological and inverse approaches, *Geochem. Geophys. Geosyst.*, 19, Q09001, doi:10.1029/2012GC004162.
- Tiberi, C., C. Ebinger, V. Ballu, G. Stuart, and B. Oluma (2005), Inverse models of gravity data from the Red Sea-Aden-East African rifts triple junction zone, *Geophys. J. Int.*, 163, 775–787, doi:10.1111/j.1365-246X.2005.02736.x.
- Tsige, L., and E. Hailu (2007), Geological Map of Bure, *EIGS*.
- Turcotte, D. L., and G. Schubert (1982), *Geodynamics: Applications of Continuum Physics to Geological Problems*, John Wiley, New York.
- Wegmann, K. W., et al. (2007), Position of the Snake River watershed divide as an indicator of geodynamic processes in the greater Yellowstone region, western North America, *Geosphere*, 3(4), 272–281.
- Weissel, J., A. Malinverno, and D. Harding (1995), Erosional development of the Ethiopian Plateau of Northeast Africa from fractal analysis of topography, in *Fractals in Petroleum Geology and Earth Processes*, edited by C. C. Barton and P. R. Pointe, pp. 127–142, Plenum Press, New York.
- Weissel, J. K., and G. D. Karner (1989), Flexural uplift of rift flanks due to mechanical unloading of the lithosphere during extension, *J. Geophys. Res.*, 94, 13,919–13,950, doi:10.1029/JB094iB10p13919.
- Wichura, H., R. Bousquet, R. Oberhänsli, M. R. Strecker, and M. H. Trauth (2010), Evidence for middle Miocene uplift of the East African Plateau, *Geology*, 38, 543–546, doi:10.1130/G31022.1.
- Wobus, C., K. X. Whipple, E. Kirby, N. Snyder, J. Johnson, K. Spyropolou, B. Crosby, and D. Sheehan (2006), Tectonics from topography: Procedures, promise, and pitfalls, *Geol. Soc. Am., Spec. Pap.*, 398, 55–74.
- Wolfenden, E., G. Yirgu, C. J. Ebinger, A. Deino, and D. Ayalew (2004), Evolution of the northern Main Ethiopian rift: Birth of a triple junction, *Earth Planet. Sci. Lett.*, 224, 213–228, doi:10.1016/j.epsl.2004.04.022.
- Wolfenden, E., C. J. Ebinger, G. Yirgu, P. Renne, and S. P. Kelley (2005), Evolution of the southern Red Sea rift: Birth of a magmatic margin, *Geol. Soc. Am. Bull.*, 117, 846–864.
- Zanettin, B., E. Justin-Visentin, M. Nicoletti, and E. Piccirillo (1980), Correlation among Ethiopian volcanic formations with special reference to the chronological and stratigraphical problems of the “Trap series”, *Atti Convegno Lincei*, 47, 231–252.
- Zenebe, B., and D. H. Mariam (2011), Geological map of Yifag area, *EIGS*.
- Zumbo, V., G. Feraud, H. Bertrand, and G. Chazot (1995), ⁴⁰Ar/³⁹Ar chronology of the tertiary magmatic activity in Southern Yemen during the early Red Sea-Aden rifting, *J. Volcanol. Geotherm. Res.*, 65, 265–279.